

François Méot
Collider-Accelerator Department
Brookhaven National Laboratory

An introduction to **Fixed Field Alternating Gradient Accelerators**

Contents

1	Introduction	5
2	MURA electron FFAGs	7
3	Mid-1960s to late 1990s	24
4	The Neutrino Factory - a source of innovations	26
5	KEK proton prototypes	27
6	KURRI KUCA	29
7	ERIT	31
8	PRISM	32
9	RACCAM	33
10	Straight S-FFAG line	34
11	EMMA	35
12	A bestiary of FFAG design studies	38

Bibliography

References

- [1] O CAMELOT ! A Memoir Of The MURA Years (Section 7.1), F.T.Cole, Proc. Cycl. Conf, April 11, 1994 ; FFAG particle accelerators, K.R. Symon et als., Phys.Rev. Vol.103-6, 1837-1859, 1956.
- [2] Fermilab repository : <http://ccdf.fnal.gov/techpubs/fermilab-reports-mura.html>
- [3] The FFAG workshops series : <https://www.bnl.gov/ffag17/pastWorkshops.php>
- [4] Engines of Discovery, A. Sessler, E. Wilson, World Scientific (2007).
- [5] Innovation Was Not Enough, L. Jones et al., World Scientific (2010).
- [6] The Development of High Energy Accelerators, M. Stanley Livingston, Dover Pubs. Inc., NY (1966).
- [7] The rebirth of the FFAG, M. Craddock, CERN Courier 44-6 (2004), <http://cerncourier.com/main/article/44/6/17>.
- [8] The FFAG synchrotron Mark I, K.R. Symon, MURA-KRS-6 (Nov. 1954)
- [9] A FFAG accelerator with spirally ridged poles, D.W. Kerst et als., MURA-DWK/KMT/LWJ/KRS-3, 1954.
- [10] The MURA 50 MeV electron accelerator, The MURA Staff, Rev. Sci. Instr., pp. 1393-1482, Vol. 35, No. 11.
- [11] Development of a FFAG proton synchrotron, M. Aiba et als., EPAC 2000.
- [12] High field-gradient cavities loaded with magnetic alloys, C. Ohmori, Procs. PAC99 (New York, 1999).
- [13] A 150 MeV FFAG synchrotron with return-yoke free magnet, T. Adachi et als., PAC01.
- [14] Y. Ishi et al., KURRI FFAG's FUTURE PROJECT AS ADS-R PROTON DRIVER, THC01, Proceedings of Cyclotrons2016, Zurich, Switzerland.
- [15] FFAGs as Accelerators and Beam Delivery Devices for Ion Cancer Therapy, D. Trbojevic, Reviews of Accelerator Science and Technology Volume 02, Issue 01, 2009.
- [16] STUDY OF FFAG-ERIT NEUTRON SOURCE, K.Okabe et al., MOPEB064, Proc. IPAC10, Kyoto, Japan.

- [17] SIX-SECTOR FFAG RING TO DEMONSTRATE BUNCH ROTATION FOR PRISM, A. Sato et al., THPP007, proceedings of EPAC08, Genoa, Italy.
- [18] J. B. Lagrange, FFAG scaling FFAG experiment, PhD dissertation, Kyoto University (2012).
- [19] Design of a spiral lattice, variable energy protontherapy FFAG, NIM A 604 (2009) 435-442 ; NIM A A 602 (2009) 293305 ; Physics Procedia 66 (2015) 361 - 369.
- [20] 8 GeV FFAG for MI, W. Chou, FFAG03 workshop (WG1), http://hadron.kek.jp/FFAG/FFAG03_HP/index.html.
- [21] Lattice optimization of FFAGs, Carol Johnstone, S. Koscielniak, Wrkshp FFAG-2004, TRIUMF, <http://www.triumf.ca/ffag2004/>.
- [22] A Feasibility Study of A Neutrino Factory in Japan, NufactJ Working Group, May 24, 2001
- [23] Studies of a European Neutrino Factory Complex, Eds. A. Blondel et als., Yellow Report CERN-2004-002.
- [24] Feasibility Study-II of a Muon-Based Neutrino Source, ed., S. Ozaki et als., BNL-52623 (2001).
- [25] Review of Current FFAG Lattice Studies in North Am., J.S. Berg et als., 17th Int. Conf. Cyclotrons (Tokyo, 2004).
- [26] Mechanisms for nonlinear accel. in FFAGs with fixed RF, S. Koscielniak, C. Johnstone, NIM A 523 (2004) 25-49.
- [27] Optimization of 1.5 GeV Proton FFAG, Sandro Ruggiero, Wrkshp FFAG-2004, TRIUMF ; Design of a non-scaling FFAG accelerator for proton-carbon therapy, D. Trbojevic et als., 17th Int. Conf. Cyclotrons (Tokyo, 2004).
- [28] Acceleration in the linear non-scaling fixed-field alternating-gradient accelerator EMMA, S. Machida, et al., Nature Physics 8, 243247 (2012).
- [29] S. Brooks, NS-FFAG arc experiment at the ATF, BNL, 2017.

1 Introduction

• Today's status

◊ Eleven FFAG rings have been operated up to now :

- 3 electron rings by MURA, 1953 - 1967 [1, 8, 9, 10]
- 2 proton rings at KEK, 500 keV and 150 MeV, 1999 - 2003 (the latter, moved to Kyushu, 2005) [11, 13]
- a 150 MeV 3-ring cascade at KURRI, for ADS-R R&D, 2005 on [14]
- an internal-target storage ring for n production, KURRI, 2007 [16]
- PRISM, a muon source, Osaka University [17]
- EMMA electron NS-FFAG, 10-20 MeV, Daresbury, 2007 - 2012 [28]

◊ in addition, have been operated in the recent past

- a prototype spiral FFAG dipole at SIGMAPHI, 2009, as part of RACCAM protontherapy FFAG study, 2005-2010 [19]
- a scaling FFAG straight section at KURRI, 2012 [18]
- a prototype NS-FFAG arc at BNL, 2017 [29]

◊ There has been a number of design and prototyping studies in the recent past :

- muon acceleration in the Neutrino Factory [22, 23, 24]
- superconducting FFAG magnets [3]
- proton drivers for ADS [20, 27]
- medical application [15, 16, 19]
- eRHIC recirculator arcs,
- CBETA now
- and more...

• The landscape at the birth of the FFAG concept, 1953

Background : nuclear physics research

- High-voltage generator : Cockcroft-Walton, 1930-32 (0.7 MV), Van de Graaf, 1929-30 (1.5 MV in 1931, ultimate 25 MV)
- Cyclotron (classical) : E.O. Lawrence, 1928-32
- Isochronous cyclotron : Thomas, 1938 (590 MeV, 1.4 MW at PSI today ; medical and isotope cyclotrons all over the planet)
- betatron : Kerst, 1940 (2.2 MeV ; ultimate 300 MeV, 1950)
- synchro-cyclotron : McMillan, 1946 (ultimate 720 MeV, Berkeley, 1957 ; 600 MeV, CERN, 1957-1990)
- Alvarez RF-linac, 1946
- pulsed synchrotron (concept Oliphant, 1943 ; electron POP UK 1945) ; led to the weak focusing Cosmotron (3.3 GeV, BNL, 1953), Bevatron (6.2 GeV, Berkeley, 1954), Synchro-Phasotron (10 GeV, Dubna, 1957)
- electron linacs, 1947 (following from high power, high frequency RF system developments)

◊ In terms of beam optics and acceleration :

- transverse focusing (cyclotron)
- isochronous acceleration (cyclotron, betatron)
- phase focusing, McMillan and Veksler (synchro-cyclotron, synchrotron)
- strong, AG focusing, Christofilos, 1950 and Courant, Livingston, Snyder, 1952 (led to CERN PS, 30 GeV, 1959, and BNL AGS, 1960)
- separated focusing (applied to synchrotron, linac)

◊ And then came the FFAG...

a quasi-simultaneous T. Ohkawa in Japan, K. Symon and D. Kerst in the United States, A. Kolomensky in USSR, ~1953

2 MURA electron FFAGs

- Motivations for MURA, in the early 1950s

- Stimulate accelerator R/D for high energy physics, and build accelerators ! in the Midwest
 - Explore alternate routes to AG synchrotrons, high intensities

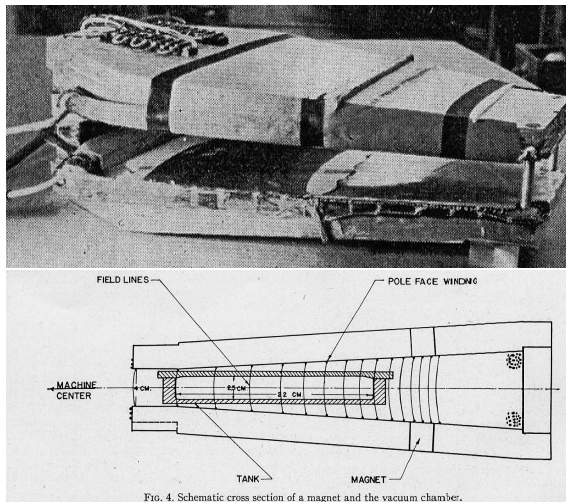
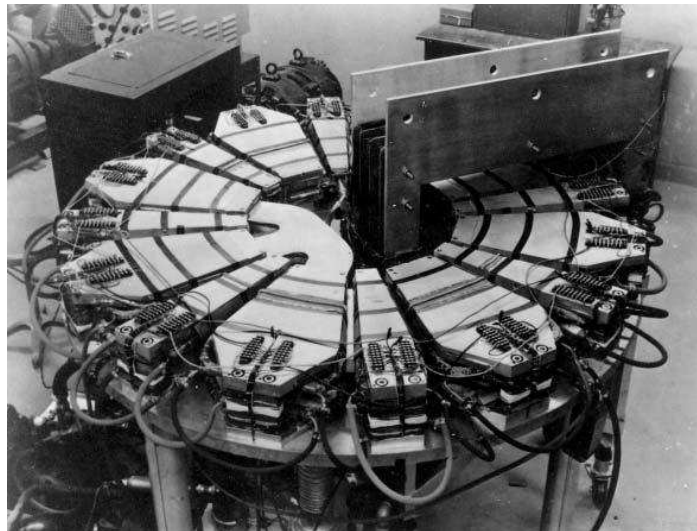
- A major contribution to accelerator science [1]

- (i) beam stacking ,
- (ii) Hamiltonian theory of longitudinal motion ,
- (iii) colliding beams (in itself a quite old idea),
- (iv) storage rings (independently invented by O'Neill),
- (v) spiral-sector geometry used in isochronous cyclotrons,
- (vi) lattices with zero-dispersion and low- β sections for colliding beams,
- (vii) multturn injection into a strong-focusing lattice,
- (viii) first calculations of the effects of nonlinear forces in accelerators ,
- (ix) first space-charge calculations including effects of the beam surroundings,
- (x) first experimental measurement of space-charge effects,
- (xi) theory of negative-mass and other collective instabilities and correction systems,
- (xii) the use of digital computation in design of orbits, magnets, and rf structures,
- (xiii) proof of the existence of chaos in digital computation, and
- (xiv) synchrotron-radiation rings

• The first model, radial sector FFAG, “MARK I”

- ◊ Main features : fixed field ring, $B = B_0(r/r_0)^K \mathcal{F}(\theta)$, strong focusing, scaling gap
- ◊ Objectives : demonstrate the FFAG principle. Studies included optics, injection, RF manipulations, effects of misalignments, exploring resonances.

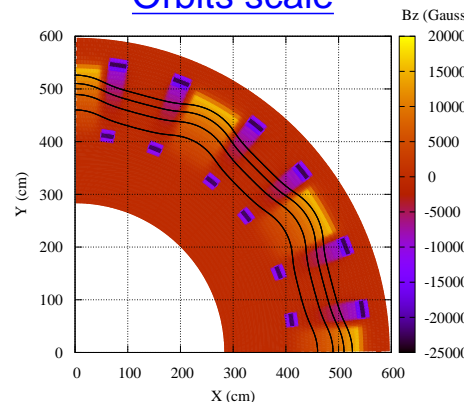
FFAG ring parameters



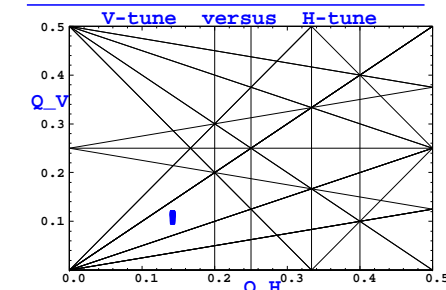
F magnet, $B > 0$, H-focusing
scaling gap $g \propto r$

$E_{inj} - E_{max}$	keV	25 - 400	$\left\{ \begin{array}{l} \text{small size, easy to build} \\ \mathcal{B}\rho/10^{-3} : 0.54 \rightarrow 2.52 \end{array} \right.$
orbit radius ($\mathcal{C}/2\pi$)	m	0.34 - 0.50	
<u>Optics</u>			
lattice	FD		
number of cells	8		4.41 deg. drifts
field index K	3.36		$g \propto r$ & pole-face windings
ν_r / ν_z	2.2-3 / 1-3		
<u>Magnet</u>			
θ_F, θ_D	deg	25.74, 10.44	sector angles
<u>Acceleration</u>			
swing	Gauss	40 - 150	
freq. swing	... added RF system, later		
gap voltage	MHz	10 in [35, 75] MHz	
	V	50	

Orbits scale



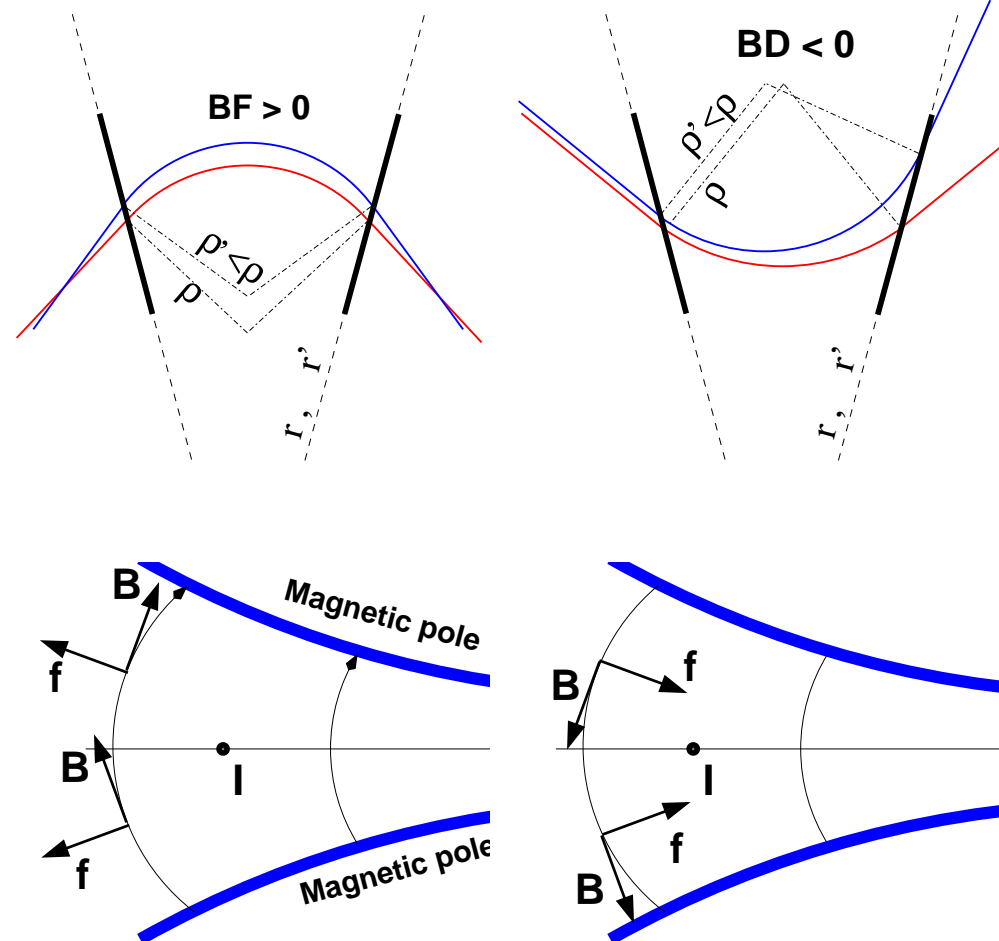
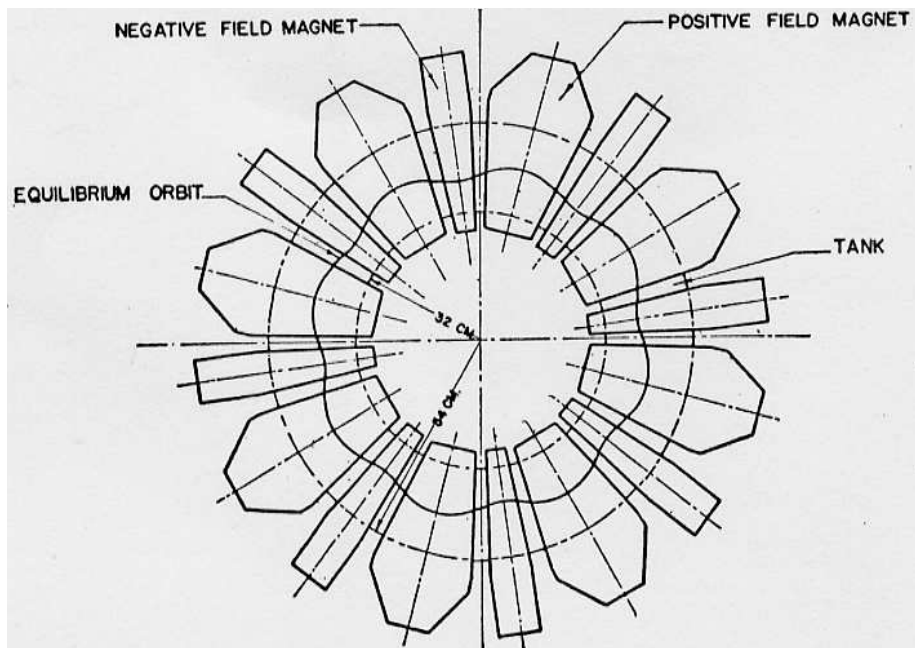
H and V tunes constant



• Basic theory

◊ Combined function optics

- A rule that yields the orientation of \vec{F} :
- $I \vec{dl}$, \vec{B} and \vec{F} , in that order, form a direct trihedra



(in this sketch I assume field obtained from pole shaping, just for simplicity)

• Solution of the motion across a combined function magnet

- ◊ A reference trajectory can be defined, characterized by $B_0\rho_0 = \frac{p_0}{q}$
- ◊ The equations of small amplitude motion ($x = \rho - \rho_0, y$) of a particle, in the Serret-Frenet frame attached to that reference curve, are derived from the Lorentz force equation

$$\frac{d\vec{p}}{dt} = q\vec{v} \times \vec{B}$$

using a transverse expansion of the magnetic field $\vec{B}(s)$ along the trajectory :

$$B_x = -n \frac{B_0}{\rho_0} y \quad [\text{+ non-linear terms}], \quad B_y = B_0 \left(1 - n \frac{x}{\rho_0}\right) \quad [\text{+ non-linear terms}]$$

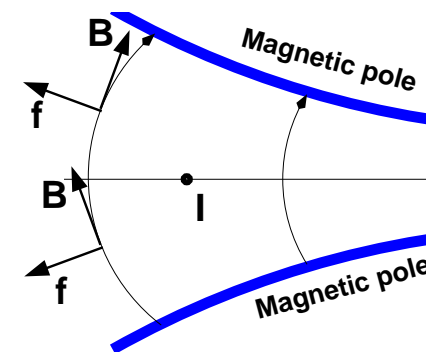
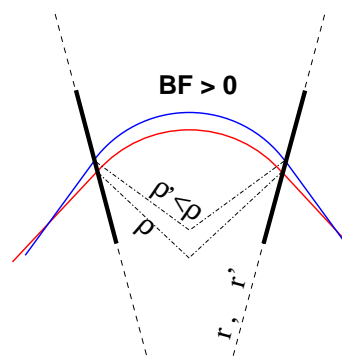
- ◊ In expanding \vec{B} the field index has been introduced :

$$n = -\frac{\rho_0}{B_0} \frac{\partial B}{\partial x}$$

The FFAG index $K = \frac{r}{B} \frac{\partial B}{\partial r}$ (of $B = B_0 \left(\frac{r}{r_0}\right)^K$) relates to
 n by $K \approx -nr/\rho$.

- ◊ Calculations (found in text books) lead to the linear approximation :

$$\begin{cases} \frac{d^2x}{ds^2} + \frac{1-n}{\rho_0^2} x = \frac{1}{\rho_0} \frac{\Delta p}{p} \\ \frac{d^2y}{ds^2} + \frac{n}{\rho_0^2} y = 0 \end{cases}$$



- HOME WORK :

What approximation leads to

$$K \approx -nR/\rho ?$$

- ◇ Solving these two differential equations yields the coordinates across a magnet (with $\mathcal{L} = (s - s_0)$ being the path length along the trajectory arc) :

Radial motion

if $(1 - n) > 0$:

$$\begin{cases} x = x_0 \cos \frac{\sqrt{1-n}}{\rho_0} \mathcal{L} + \frac{x'_0}{\sqrt{1-n}} \sin \frac{\sqrt{1-n}}{\rho_0} \mathcal{L} + \frac{\rho_0}{\sqrt{1-n}} (1 - \cos \frac{\sqrt{1-n}}{\rho_0} \mathcal{L}) \frac{\Delta p}{p} \\ x' = -x_0 \frac{\sqrt{1-n}}{\rho_0} \sin \frac{\sqrt{1-n}}{\rho_0} \mathcal{L} + x'_0 \cos \frac{\sqrt{1-n}}{\rho_0} \mathcal{L} + \frac{\rho_0}{\sqrt{1-n}} \sin \frac{\sqrt{1-n}}{\rho_0} \mathcal{L} \frac{\Delta p}{p} \end{cases}$$

if $(1 - n) < 0$:

$$\begin{cases} x = x_0 \cosh \frac{\sqrt{n-1}}{\rho_0} \mathcal{L} + \frac{x'_0}{\sqrt{n-1}} \sinh \frac{\sqrt{n-1}}{\rho_0} \mathcal{L} + \frac{\rho_0}{n-1} (1 - \cosh \frac{\sqrt{n-1}}{\rho_0} \mathcal{L}) \frac{\Delta p}{p} \\ x' = x_0 \frac{\sqrt{n-1}}{\rho_0} \sinh \frac{\sqrt{n-1}}{\rho_0} \mathcal{L} + x'_0 \cosh \frac{\sqrt{n-1}}{\rho_0} \mathcal{L} + \frac{\rho_0}{n-1} \sinh \frac{\sqrt{n-1}}{\rho_0} \mathcal{L} \frac{\Delta p}{p} \end{cases}$$

Axial motion :

if $n > 0$:

$$\begin{cases} y = y_0 \cos \frac{\sqrt{n}}{\rho_0} \mathcal{L} + \frac{y'_0}{\sqrt{n}} \sin \frac{\sqrt{n}}{\rho_0} \mathcal{L} \\ y' = -y_0 \frac{\sqrt{n}}{\rho_0} \sin \frac{\sqrt{n}}{\rho_0} \mathcal{L} + y'_0 \cos \frac{\sqrt{n}}{\rho_0} \mathcal{L} \end{cases}$$

if $n < 0$:

$$\begin{cases} y = y_0 \cosh \frac{\sqrt{-n}}{\rho_0} \mathcal{L} + \frac{y'_0}{\sqrt{-n}} \sinh \frac{\sqrt{-n}}{\rho_0} \mathcal{L} \\ y' = y_0 \frac{\sqrt{-n}}{\rho_0} \sinh \frac{\sqrt{-n}}{\rho_0} \mathcal{L} + y'_0 \cosh \frac{\sqrt{-n}}{\rho_0} \mathcal{L} \end{cases}$$

◊ In transport matrix notations (with, for short, $k_x = |1 - n|/\rho_0^2$, $k_y = |n|/\rho_0^2$)

If $n < 0$: The dipole is horizontally focusing and vertically defocusing

$$\begin{pmatrix} x \\ x' \\ y \\ y' \\ \frac{\delta p}{p} \end{pmatrix} = \begin{pmatrix} \cos \sqrt{k_x} \mathcal{L} & \frac{1}{\sqrt{k_x}} \sin \sqrt{k_x} \mathcal{L} & 0 & 0 & \frac{1}{\rho k_x} (1 - \cos \sqrt{k_x} \mathcal{L}) \\ -\sqrt{k_x} \sin \sqrt{k_x} \mathcal{L} & \cos \sqrt{k_x} \mathcal{L} & 0 & 0 & \frac{1}{\rho \sqrt{k_x}} \sin \sqrt{k_x} \mathcal{L} \\ 0 & 0 & \cosh \sqrt{k_y} \mathcal{L} & \frac{1}{\sqrt{k_y}} \sinh \sqrt{k_y} \mathcal{L} & 0 \\ 0 & 0 & \sqrt{k_y} \sinh \sqrt{k_y} \mathcal{L} & \cosh \sqrt{k_y} \mathcal{L} & 0 \\ 0 & 0 & 0 & 0 & 1 \end{pmatrix} \begin{pmatrix} x_0 \\ x'_0 \\ y_0 \\ y'_0 \\ \frac{\delta p}{p} \end{pmatrix}$$

If $0 < n < 1$: The dipole is focusing in both planes. aka “weak focusing” (cyclotrons)

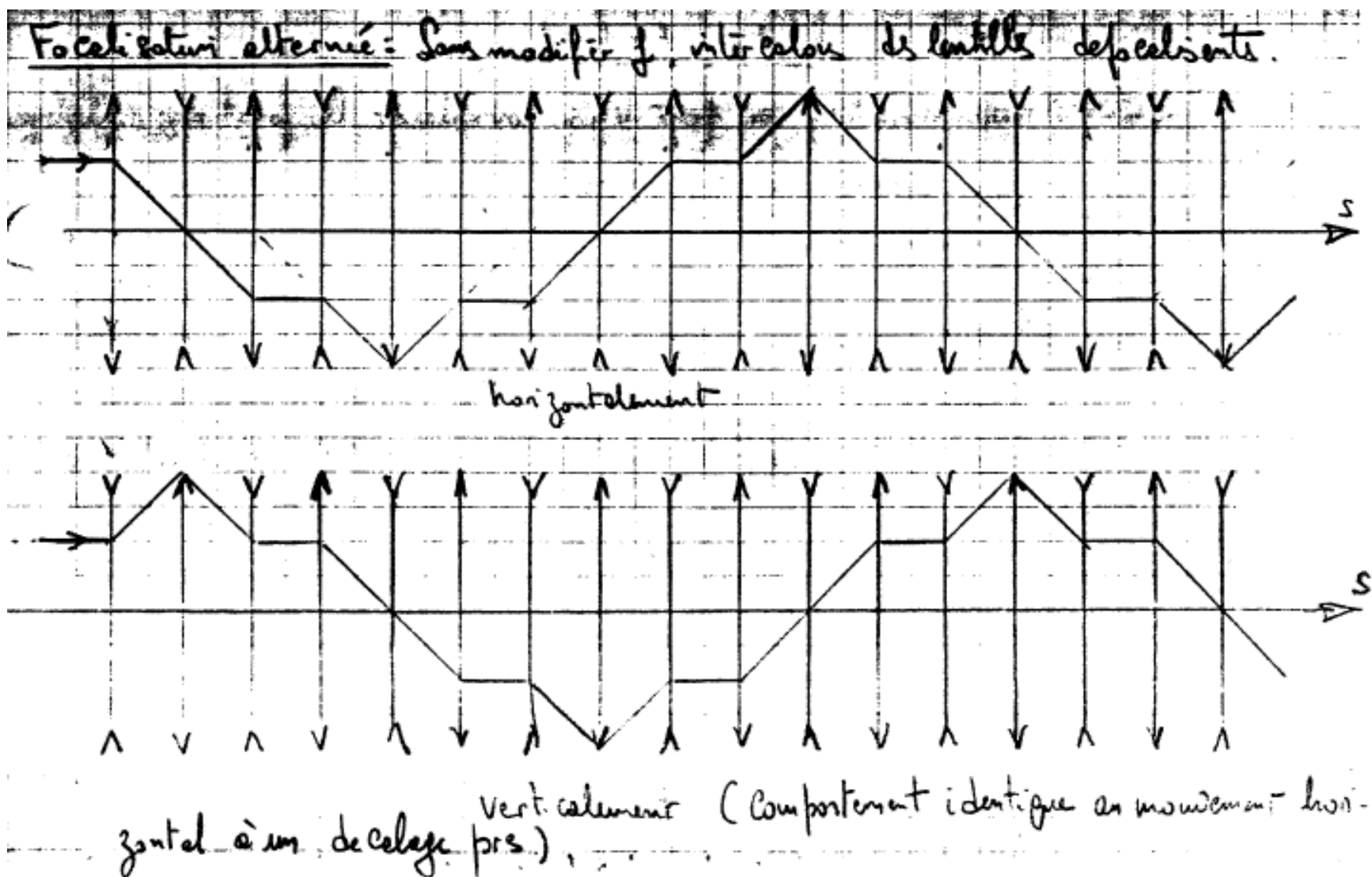
$$\begin{pmatrix} x \\ x' \\ y \\ y' \\ \frac{\delta p}{p} \end{pmatrix} = \begin{pmatrix} \cos \sqrt{k_x} \mathcal{L} & \frac{1}{\sqrt{k_x}} \sin \sqrt{k_x} \mathcal{L} & 0 & 0 & \frac{1}{\rho k_x} (1 - \cos \sqrt{k_x} \mathcal{L}) \\ -\sqrt{k_x} \sin \sqrt{k_x} \mathcal{L} & \cos \sqrt{k_x} \mathcal{L} & 0 & 0 & \frac{1}{\rho \sqrt{k_x}} \sin \sqrt{k_x} \mathcal{L} \\ 0 & 0 & \cos \sqrt{k_y} \mathcal{L} & \frac{1}{\sqrt{k_y}} \sin \sqrt{k_y} \mathcal{L} & 0 \\ 0 & 0 & -\sqrt{k_y} \sin \sqrt{k_y} \mathcal{L} & \cos \sqrt{k_y} \mathcal{L} & 0 \\ 0 & 0 & 0 & 0 & 1 \end{pmatrix} \begin{pmatrix} x_0 \\ x'_0 \\ y_0 \\ y'_0 \\ \frac{\delta p}{p} \end{pmatrix}$$

If $n > 1$: The dipole is horizontally defocusing and vertically focusing.

$$\begin{pmatrix} x \\ x' \\ y \\ y' \\ \frac{\delta p}{p} \end{pmatrix} = \begin{pmatrix} \cosh \sqrt{k_x} \mathcal{L} & \frac{1}{\sqrt{k_x}} \sinh \sqrt{k_x} \mathcal{L} & 0 & 0 & \frac{1}{\rho k_x} (1 - \cosh \sqrt{k_x} \mathcal{L}) \\ \sqrt{k_x} \sinh \sqrt{k_x} \mathcal{L} & \cosh \sqrt{k_x} \mathcal{L} & 0 & 0 & \frac{1}{\rho \sqrt{k_x}} \sinh \sqrt{k_x} \mathcal{L} \\ 0 & 0 & \cos \sqrt{k_y} \mathcal{L} & \frac{1}{\sqrt{k_y}} \sin \sqrt{k_y} \mathcal{L} & 0 \\ 0 & 0 & -\sqrt{k_y} \sin \sqrt{k_y} \mathcal{L} & \cos \sqrt{k_y} \mathcal{L} & 0 \\ 0 & 0 & 0 & 0 & 1 \end{pmatrix} \begin{pmatrix} x_0 \\ x'_0 \\ y_0 \\ y'_0 \\ \frac{\delta p}{p} \end{pmatrix}$$

◊ “MARK I” uses strong focusing, BF is focusing, BD is defocusing

- The (BF,BD) doublet is globally focusing in both x and y planes :



- ◇ Wedge focusing is required to complete the (BF,BD) cell matrix
 - It stems from the orbit geometry :

The following geometrical relationships are evident from the figure, where N is the total number of sectors, and the approximate expressions are valid when the angles are small:

$$N = \frac{2\pi}{\beta_1 + \beta_2} = \frac{2\pi}{\theta_1 + \theta_2} \quad (1)$$

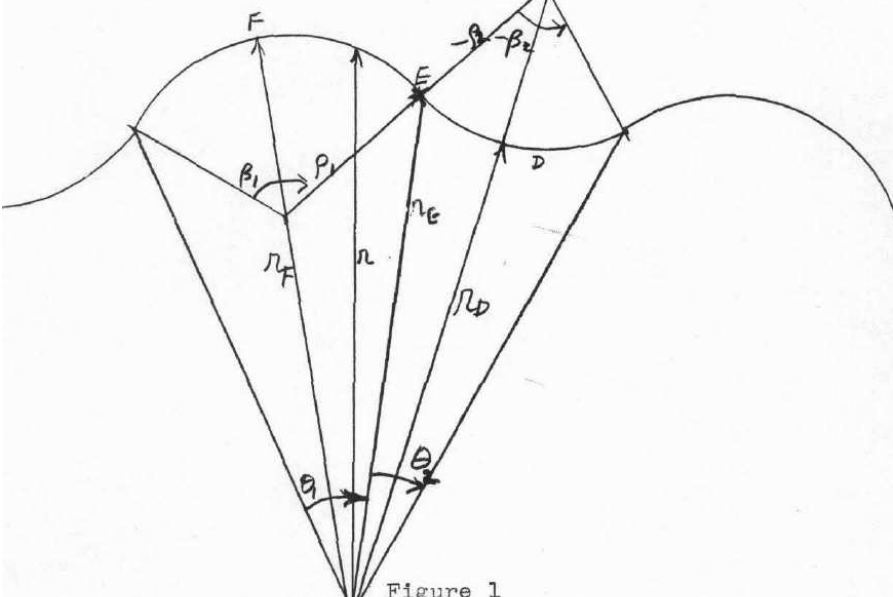


Figure 1

$$\rho = r_E \frac{\sin \theta_2}{\sin \beta_2} \doteq r \frac{\theta_2}{\beta_2} \quad (2)$$

(either sector)

The length of either sector is

$$S = \rho \beta \doteq r \theta \quad (3)$$

The total length of orbit is

$$L = N(S_1 + S_2) = 2\pi \frac{\beta_1 \rho_1 + \beta_2 \rho_2}{\beta_1 + \beta_2} \quad (4)$$

K.R. Symon, The FFAG synchrotron MARK I, MURA-KRS-6 (1954)

◊ MARK I is a ring, one more ingredient is needed to make it operational :
periodic stability

- Let's oversimplify : we forget drifts, wedge focusing,
- let's also consider magnets with same field ($B_{0,F} = B_{0,D}$) and same index ($k_F = k_D = k$),
- thus the transport matrix for the (BF,BD) cell writes :

$$\begin{pmatrix} \cosh \sqrt{k_D} \mathcal{L}_D & \frac{1}{\sqrt{k_D}} \sinh \sqrt{k_D} \mathcal{L}_D \\ \sqrt{k_D} \sinh \sqrt{k_D} \mathcal{L}_D & \cosh \sqrt{k_D} \mathcal{L}_D \end{pmatrix} \times \begin{pmatrix} \cos \sqrt{k_F} \mathcal{L}_F & \frac{1}{\sqrt{k_F}} \sin \sqrt{k_F} \mathcal{L}_F \\ -\sqrt{k_F} \sin \sqrt{k_F} \mathcal{L}_F & \cos \sqrt{k_F} \mathcal{L}_F \end{pmatrix} =$$

$$\begin{pmatrix} \cosh \sqrt{k} \mathcal{L}_D \times \cos \sqrt{k} \mathcal{L}_F - \sinh \sqrt{k} \mathcal{L}_D \times \sin \sqrt{k} \mathcal{L}_F & (*) \\ (*) & \sinh \sqrt{k} \mathcal{L}_D \times \sin \sqrt{k} \mathcal{L}_F + \cosh \sqrt{k} \mathcal{L}_D \times \cos \sqrt{k} \mathcal{L}_F \end{pmatrix}$$

- Periodic stability requires

$$\frac{1}{2} \text{Trace}[CellMatrix] < 1 \quad - \text{for both planes !}$$

i.e.,

$$\cosh \sqrt{k} \mathcal{L}_D \times \cos \sqrt{k} \mathcal{L}_F < 1 \quad \text{and} \quad \cos \sqrt{k} \mathcal{L}_D \times \cosh \sqrt{k} \mathcal{L}_F < 1 \quad (\text{noting } \sqrt{k} \mathcal{L} = \sqrt{k} \mathcal{L})$$

- HOME WORK :

Plot the stability diagram, *i.e.*, the region of periodic stability in the $(\sqrt{k}\mathcal{L}_F, \sqrt{k}\mathcal{L}_D)$ space (take $\sqrt{k}\mathcal{L}_F \in [0, 2\pi]$, $\sqrt{k}\mathcal{L}_D \in [0, 2\pi]$).

• Constant tunes

- ◊ Re-write the linearized equation of motion (slide #2) with the transformation $s = r \theta$ yields

$$\frac{d^2x}{d\theta^2} + \left(\frac{r(\theta)^2}{\rho^2(r, \theta)} [1 - n] \right) x = 0$$

$$\frac{d^2y}{d\theta^2} + \left(\frac{r(\theta)^2}{\rho^2(r, \theta)} n \right) y = 0$$

(r is the local radius of the trajectory wrt center of the ring, ρ is the local curvature radius).

- ◊ Thus, two sufficient conditions to have both the vertical and horizontal betatron oscillations constant with respect to the momentum (*i.e.*, the forcing terms in the above equations constant), are:

$$\frac{\partial n}{\partial p} \Big|_{\theta=const} = 0$$

$$\frac{\partial}{\partial p} \left(\frac{r}{\rho} \right) \Big|_{\theta=const} = 0$$

- the first one expresses the constancy of the field index with respect to the momentum
- the second one expresses the similarity of the closed orbits.

This defines a “zero-chromaticity” optics :

$$\frac{\delta\nu}{\delta p/p} = 0 \tag{1}$$

- HOME WORK :

Show that, with the FFAG scaling law $B = B_0(r/r_0)^K \mathcal{F}(\theta)$,
this happens.

(take a step function for $\mathcal{F}(\theta)$: 1 inside the magnets, 0 outside)

• Longitudinal motion, longitudinal stability

- ◊ If synchrotron style of RF operation is used, then the longitudinal motion satisfies the regular phase-stability principles,

$$\Phi'' + \frac{\Omega^2}{\cos \phi_s} (\sin \phi - \sin \phi_s) = 0$$

synchrotron frequency $f_s = \Omega_s/2\pi = \frac{c}{\mathcal{L}} \left(\frac{h\eta \cos \phi_s q \hat{V}}{2\pi E_s} \right)^{1/2}$, bucket height $\pm \frac{\Delta p}{p} = \pm \frac{1}{\beta_s} \left(\frac{2q\hat{V}}{\pi h\eta E_s} \right)^{1/2}$, etc.

• Betatron damping

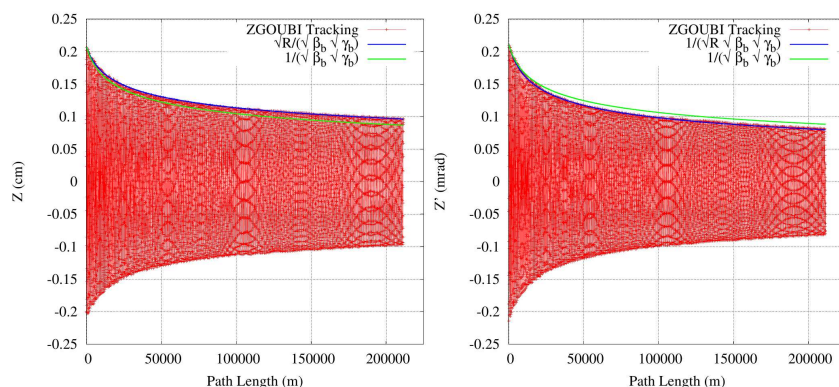
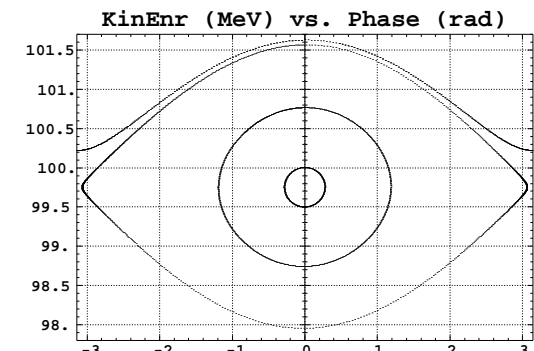
Introducing the velocity term and its variation, the previous differential

equations change to :

$$\begin{aligned} x'' + \frac{(\beta\gamma)'}{\beta\gamma} x' + \frac{1-n}{\rho_0^2} x &= \frac{1}{\rho_0} \frac{\Delta p}{p} \\ y'' + \frac{(\beta\gamma)'}{\beta\gamma} y' + \frac{n}{\rho_0^2} y &= 0 \end{aligned}$$

Solving (text books ...) yields (same for y, y')

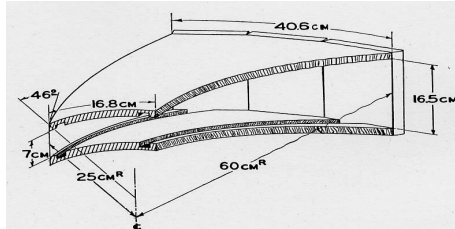
$$x \propto \sqrt{\frac{r}{\beta\gamma}}, \quad x' \propto \sqrt{\frac{1}{r \times \beta\gamma}}$$



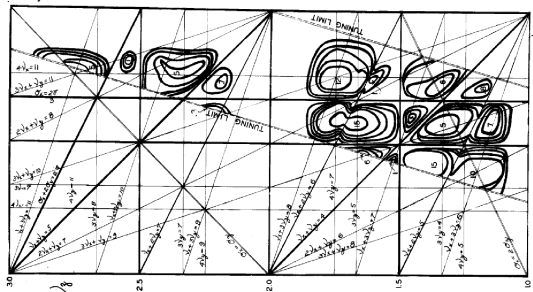
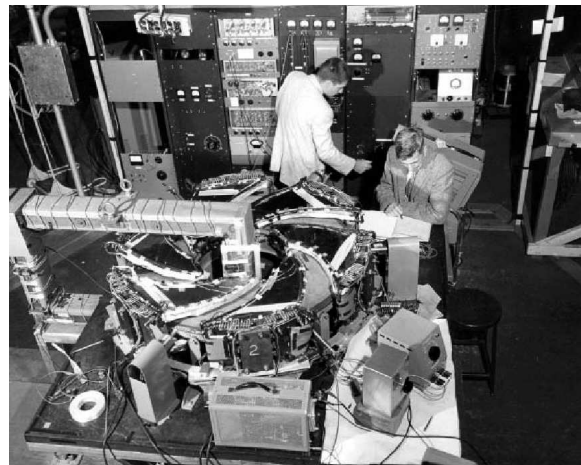
• Second model, spiral sector FFAG, “MARK V”

- ◊ The idea in the spiral FFAG was to avoid the “wrong sign” curvature and bring the circumference factor $C = R/\rho$ close to 1. The wedge angles provides the vertical focusing.
- ◊ R&D objectives : spiral FFAG POP - first extensive use of computers to determine magnetic field and machine parameters ; long-term orbit stability ; RF acceleration methods.

First operation Aug. 1957 at the MURA Lab., Madison.



Spiral dipole, $B > 0$,
H-focusing
scaling gap g_{cr}



Injection

Acceleration

MARK V PARAMETERS

$E_{\text{inj}} - E_{\text{max}}$	keV	35 - 180	{ reasonable size magnets}
orbit radius	m	0.34 - 0.52	spiraling orbit
$E_{\text{tr}} / r_{\text{tr}}$	keV/m	155 / 0.49	{ RF exprmnts at $\gamma_{\text{tr}} = (1 + K)^{1/2}$ }
<u>Optics</u>	strong focusing, scaling		
lattice	N spiral sectors		
number of sectors	6		
field index K	0.7		
flutter F_{eff}	1.1		
ν_r / ν_z	1.4 / 1.2		
β_r / β_z	tunable min-max		
<u>Magnet</u>	0.45-1.3 / 0.6-1.4		
ζ	spiral sector, $B = B_0 \left(\frac{r}{r_0}\right)^K \mathcal{F}(N(\tan \zeta \ln \frac{r}{r_0} - \theta))$		
gap	deg	46	edge to radius angle
	cm	16.5 - 7	$g/r = Cte$
<u>Injection</u>	cont. or pulsed		
<u>Acceleration</u>	betatron and RF		
	extensive RF tests		

Figure 4: Resonance Survey, Radial Sector Model

• On the optics in the spiral FFAG

- ◊ The following form for the field preserves the scaling property in an N-periodic spiral FFAG:

$$B(r, \theta)|_{z=0} = B_0 \left(\frac{r}{r_0} \right)^K \mathcal{F} \left(N(\tan \zeta \times \ln \frac{r}{r_0} - \theta) \right)$$

\mathcal{F} is the axial modulation of the field (“flutter”). One can for instance think of

$$\mathcal{F} = 1 + f \sin \left(N(\tan \zeta \ln \frac{r}{r_0} - \theta) \right), f \approx 0.25.$$

- The logarithmic spiral edge ($r = r_0 \exp((\theta - \theta_0)/\tan \zeta)$) ensures constant angle between spiral sector edges and radius.
- The in and out wedge angles are different, V-defocusing, and V-focusing (larger), overall effect is vertical focusing.

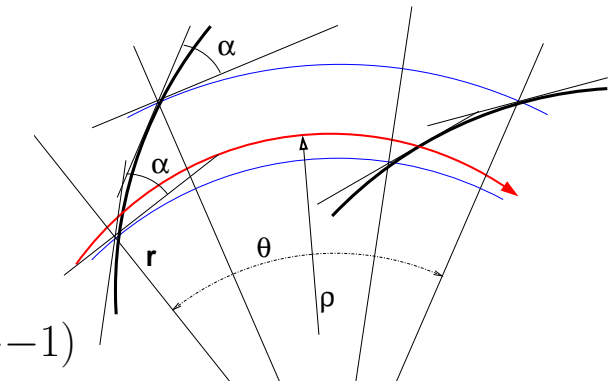
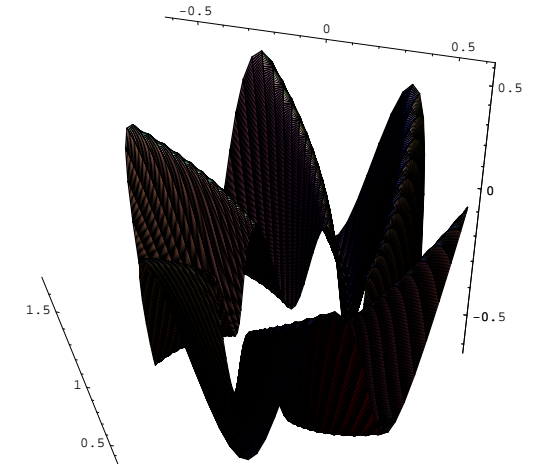
- ◊ Effect field fall-off extent on vertical focusing

$$\begin{pmatrix} x \\ x' \end{pmatrix} = \begin{pmatrix} 1 & 0 \\ \frac{\tan \epsilon}{\rho} & 1 \end{pmatrix} \begin{pmatrix} x_0 \\ x'_0 \end{pmatrix}, \begin{pmatrix} y \\ y' \end{pmatrix} = \begin{pmatrix} 1 & 0 \\ -\frac{\tan(\epsilon-\psi)}{\rho} & 1 \end{pmatrix} \begin{pmatrix} y_0 \\ y'_0 \end{pmatrix},$$

where $\psi = \frac{I_1 \cdot \lambda \cdot (1 + \sin^2(\epsilon))}{\rho \cdot \cos(\epsilon)}$, with $I_1 = \int \frac{B_z(s) \cdot (B_0 - B_z(s))}{\lambda \cdot B_0^2} \cdot ds$, λ is the fringe field extent.

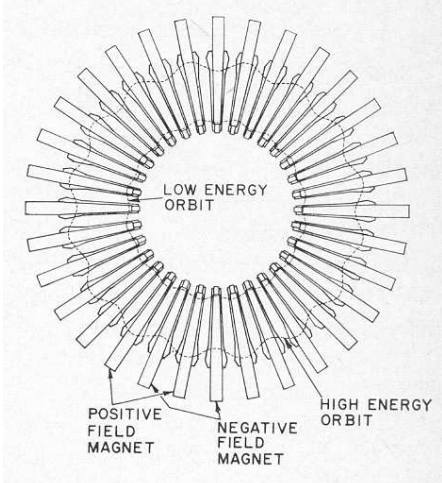
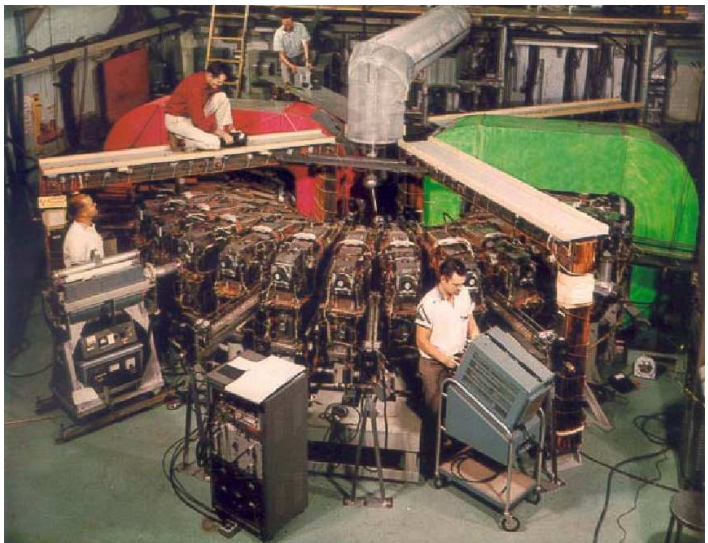
- ◊ Expansion of the equations of motion around the scalloped orbit in the linear approximation yields the approximate tunes

$$\nu_r \approx \sqrt{1 + K}, \quad \nu_z \approx \sqrt{-K + F^2(1 + 2 \tan^2 \zeta)} \quad (F = \frac{\overline{B}^2}{B^2} - 1 \xrightarrow{\text{hard-edge}} \frac{R}{\rho} - 1)$$



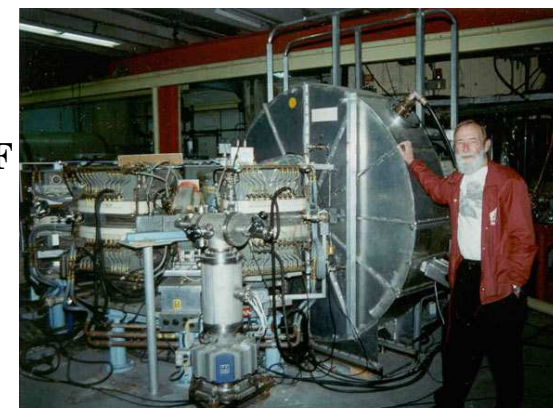
• Second radial sector, 50 MeV, 2-way

- ◊ Preliminary studies early 1957. The spiral sector e-model was not yet completed - this determined the choice of radial sector : easier to design, better understood. Pole is not scaling : $g \propto 1/r$, constant tunes require tweaking the flutter, and pole face windings.
- ◊ Study objectives : RF stacking, high circulating I , 2-way storage.
- ◊ First start Dec. 1959, 2-beam mode, 27 MeV ; disassembled in 60, magnets corrected ; second start Aug. 61, single beam, 50 MeV.



FFAG parameters

$E_{inj} - E_{max}$	MeV	0.1 - 50	<i>reasonable size & beam life-time</i> $B\rho : 0.001 \rightarrow 0.17 \text{ (T.m)}$	
orbit radius	<i>m</i>	1.20 - 2.00		
<i>Optics</i>				
lattice		FODO	$B \approx B_0(r/r_0)^K \cos(16\theta)$ 32 magnets, 3.15 deg. drifts	
number of cells		16		
K		9.25		
ν_r / ν_z		4.42 / 2.75		
<i>Magnet</i>				
θ, core	<i>deg</i>	6.3	<i>at r_{max}</i>	
peak field	<i>T</i>	0.52		
gap	<i>cm</i>	8.6		
power	<i>kW</i>	100		
<i>Injection</i>				
<i>Acceleration</i>				
swing	<i>MHz</i>	20 - 23		
harmonic		1		
voltage p-to-p	<i>kV</i>	1.3 - 3		
cycle rep. rate	<i>Hz</i>	60		



- Ended up injector to the first dedicated light source storage ring - by MURA, Tantalus.

3 Mid-1960s to late 1990s

- After MURA, reduced activity. On alternative proposals in high power proton beam projects mostly.

◊ **ESS accelerator facility** should serve two target stations, a 5MW 50 Hz and a 1MW 10Hz.

Structure : a 1.33GeV H- Linac followed by 2 accumulator rings that compress the beam pulse to $0.4\mu\text{s}$ (H- injection, 1000 turns), 2.5MW throughput each, 2.3×10^{14} ppp, 25Hz, radius 26m, lavg in each ring=63A.

Alternative FFAG scheme (early 1990's) : 0.4 GeV H- Linac followed by either 1.6 or 3 GeV FFAG.

Finally rejected, considered difficult option : injection (drifts too short), large magnets, high cost.

beam power	MW	5	
top E	GeV	3	
ppp	GeV	2×10^{14}	
rep. rate	Hz	50	. users' specif
$\langle I \rangle$	mA	1.7	
max. radius	m	45	
<i>injection</i>			. multитurn, charge exchange
E	MeV	430	. space charge tune shift constraint
# of turns		260	. $320 \mu\text{s}$
<i>extraction</i>			. single turn, fast kicker
power gain with FFAG		7	. favors lower intensity (hence higher top E and – stronger magn.)
<i>FFAG optics</i>	DFD triplet, K	21	. feasibility of the magnets was demonstrated / $\gamma_{tr} > \gamma_{max}$
	straight section length	m	10
	number of sectors		20
	ν_r / ν_z		5.8 / 2.8
	radial excursion	m	2.7
<i>RF</i>	$B_{D,min} / B_{F,max}$	T	-2 / 4
	freq	MHz	0.8 - 1
	voltage ($\times 10$ cavities)	kV	20

◊ Fermilab proton driver

[W. Chou, P.F. Meads, FFAG03]

Two options 1 : synchrotron, Linac

Possible option 3 : FFAG, because it is supposed to feature large acceptance, high repetition rate.

Two optics explored : spiral (issue of RF space) and radial (magnets and β_V too big).

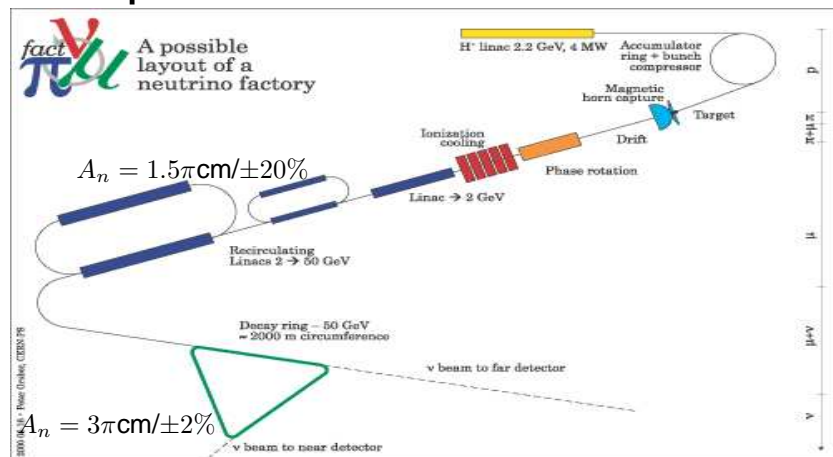
An additional drawback was : difficult to install in existing accelerator complex.

		p-Driver	FFAG radial sector	
Energy	GeV		8	. FFAG : need more than one ring ?
$E - \text{injection}$	MeV		600	
beam power	MW		0.5	
p/bunch			$3 \cdot 10^{11}$	
circumference	m		474	
optics			DFD	
# of sectors			32	
K value			120	
radial extent	m		4.55	
rep. rate	Hz	15	105	. $\times 7 \rightarrow$ Needs new Linac
b/pulse (RF harmonic)		84	12	
p/pulse		$2.5 \cdot 10^{13}$	$3.6 \cdot 10^{12}$. synchrotron $\xrightarrow{1/7}$ FFAG
RF frequency	MHz	53	7.5	. FFAG needs bunch rotation for inj. into
RF peak power	kW		200	
$< I >$	μA		60	. 7 times lower circulating current in FFA
$\beta\gamma\epsilon_{x,z}$	10^{-6}m.rad		40π	
$\beta\gamma\epsilon_l$	eV.s		0.2	
# of injections to MI (inj. time 400 ms)		6	42	. an advantage of Option 2 compared to
cost estimates	M\$	230	130	. rough, for a 0.8-2.5 GeV, 5 MW design

4 The Neutrino Factory - a source of innovations

It has triggered a strong activity in the domain of FFAG design, and lead to the development of new concepts.

Europe NuFact



US NuFact



- Study I, II ν-Factory – feasible but too expensive
- Biggest cost item: acceleration (~600M\$)

Table A.1: Construction Cost Rollup per Components for Study-II Neutrino Factory. All costs are in FY01 dollars.

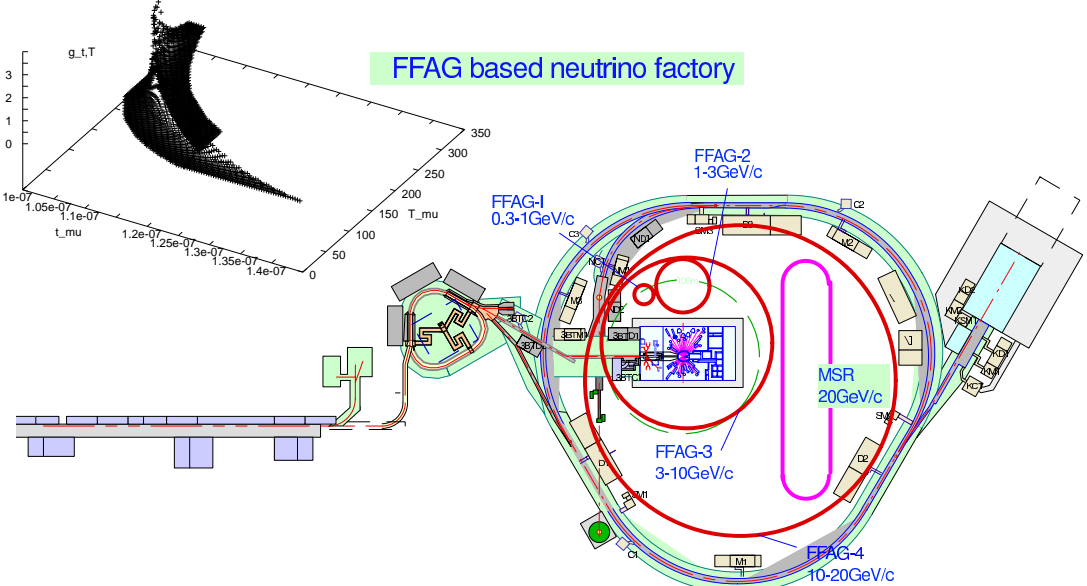
System	Magnets (\$M)	RF power (\$M)	RF cav. (\$M)	Vac. (\$M)	PS (\$M)	Diagn. (\$M)	Cryo (\$M)	Util. (\$M)	Conv. Facil. (\$M)	Sum (\$M)
Proton Driver	5.5	7.0	66.1	0.8	26.6	2.2	28.5			21.9
Target Systems	30.3			0.8	3.5	8.0	18.8			30.2
Decay Channel	3.1			0.2	0.1	1.0	0.2			4.6
Induction Linacs	35.0		90.3	4.4	163.3	3.0	3.6			19.5
Bunching	48.8	6.5	3.2	2.7	2.1	5.0	0.3			68.6
Cooling Channel	127.6	105.6	17.7	4.3	4.8	28.0	0.5			19.5
Pre-accel. linac	46.3	68.4	44.1	7.5	3.0	6.0	13.6			188.9
RLA	129.0	89.2	63.4	16.4	5.6	4.0	28.9			355.5
Storage Ring	38.5			4.8	2.2	29.0	4.8			28.1
Site Utilities								126.9		107.4
Totals	464.1	276.7	284.8	50.9	211.2	86.2	108.2	126.9	138.2	1,747.2

The Europe and the two US NuFact studies propose to accelerate muons up to the storage energy (20 or 50 GeV) by means of one or two 4- or 5-pass RLA's. RLA's are complicated machines (spreaders, combiners), hence expensive.

The Japan NuFact

J-Parc: 50-GeV, 3.3×10^{14} ppp at 0.3 Hz ($15 \mu\text{A}$) / 0.75 MW
Four muon FFAG's : 0.2-1 GeV, 1-3, 3-10 (SC), 10-20 (SC).
No cooling, compact ($R \approx 200\text{m}$)

30ns/300±50% MeV bunch



Acceleration rate is lower than RLA, requires larger distance, but, acceptance is larger both transversally (twice : DA $3 \pi\text{cm}$ norm. at $\delta p = 0$) and longitudinally ($\approx 5 \text{ eV.s}$). Hence achieve comparable production rate : $\approx 10^{20}$ muon decays per year (1 MW p power).



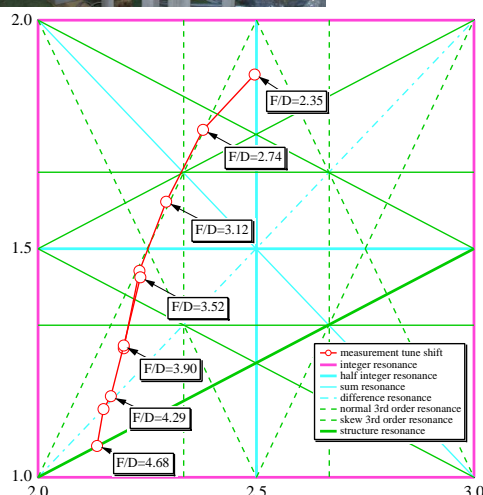
5 KEK proton prototypes

- POP - Proof of principle, the first proton FFAG

First beam Dec. 1999.

[Typical] data

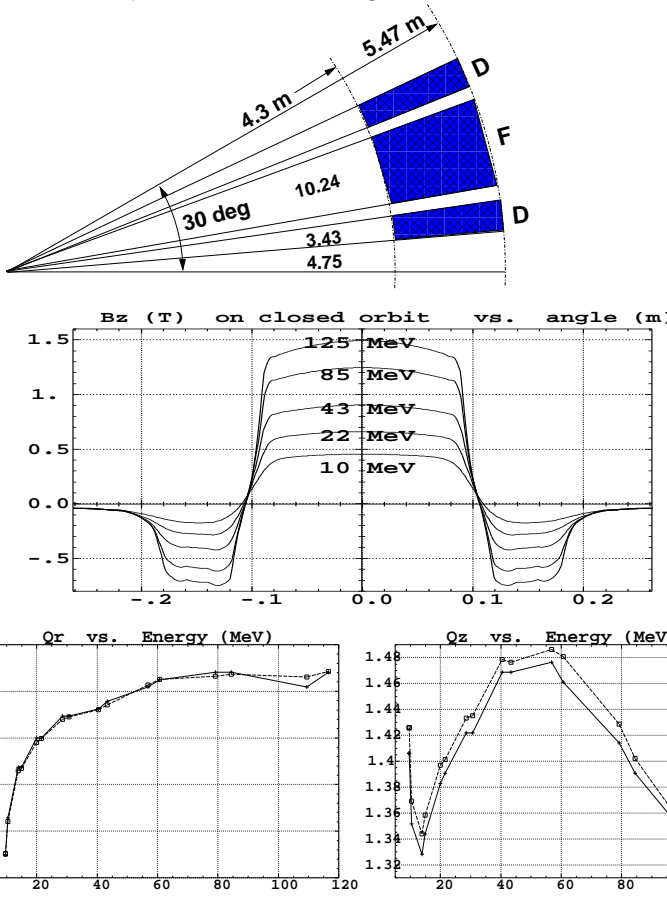
$E_{inj} - E_{max}$	keV	50 - 500	$(B = B_0(r/r_0)^K \mathcal{F}(\theta))$
orbit radius	m	0.8 - 1.14	
<i>Optics</i>			
lattice		DFD	
number of cells		8	
K		2.5	
β_r, β_z max.	m	0.7	
ν_r / ν_z		2.2 / 1.25	
<i>Magnet</i>			<i>tunable via B_F/B_D ratio</i>
θ_D / θ_F , core	deg	2.8 / 14	<i>sector triplet</i>
B_D / B_F	T	0.04-0.13 / 0.14-0.32	
gap	cm	30-9	
<i>Injection</i>			$r_{inj} \rightarrow r_{max}$
<i>Extraction</i>			$gap = g_0(r_0/r)^K$
<i>Acceleration</i>			$\left\{ \begin{array}{l} \text{electrostatic inflector} \\ + 2 \text{ bumpers} \end{array} \right.$
high field, non-linear gradient			
<i>Amorphous MA cavity</i>			
swing	MHz	0.6 - 1.4	broad band, high \vec{E} RF ; 2-beam accel.
harmonic		1	
voltage p-to-p	kV	1.3 - 3	
cycle time	ms	1	
rep. rate	kHz	1	
\dot{B}	T/s	180	
			fast acceleration
			high average current



• The 150 MeV machine



“return yoke free” magnet



First operation 2003.

[Typical] data

$E_{inj} - E_{max}$	MeV	12 - 150	
orbit radius	m	4.47 - 5.20	
<u>Optics</u>			
lattice		DFD	9.5 deg. drift
numb. of cells		12	
K		7.6	$(B = B_0(r/r_0)^K \mathcal{F}(\theta))$
β_r / β_z max.	m	2.5 / 4.5	
ν_r / ν_z		3.7 / 1.3	tunable via B_F/B_D ratio
α, γ_{tr}		0.13, 2.95	$1/(1+K), (1+K)^{1/2}$
$\mathcal{R}/\rho _{E_{max}}$		5.4	
<u>Magnet</u>			
θ_D / θ_F	deg	3.43 / 10.24	
B_D / B_F	T	0.2-0.78 / 0.5-1.63	
gap	cm	23.2 - 4.2	$r_{inj} \rightarrow r_{max}$ at $r_{inj} - r_{max}$ (gap = $g_0 \left(\frac{r_0}{r}\right)^K$)
<u>Injection</u>			$\begin{cases} B\text{-septum} + E\text{-septum} \\ + 2 \text{ bumpers} \end{cases}$
<u>Extraction</u>			
<u>Acceleration</u>			fast kicker (1kG, 150 ns)
swing	MHz	1.5 - 4.5	
harmonic		1	
voltage p-to-p	kV	2	
ϕ_s	deg	20	
ν_s		0.01 - 0.0026	
\dot{B}	T/s	300	
rep. rate	Hz	250	fast acceleration high average current

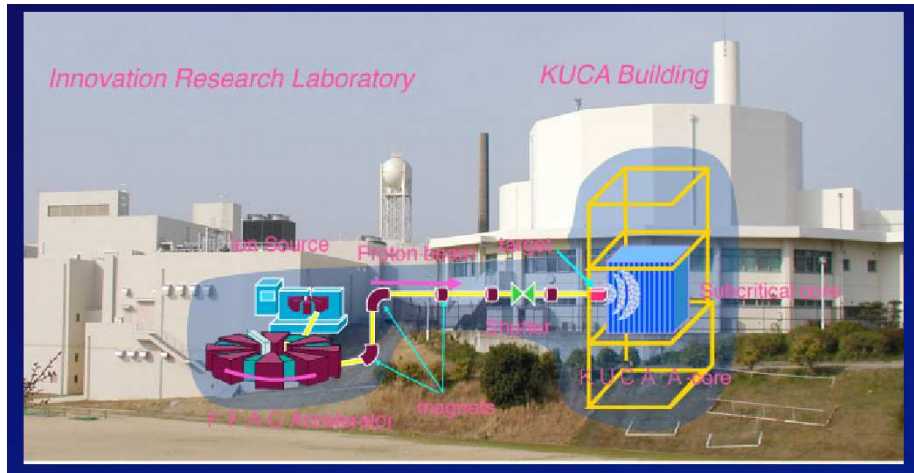
6 KURRI KUCA

An ADS-R experiments, proton driver R/D

- First coupling to an ADS-R core, March 2009, 100 MeV beam
- Thorium-loaded ADS-R experiment, March 2010 : 100 MeV, 30 Hz, 5 mW

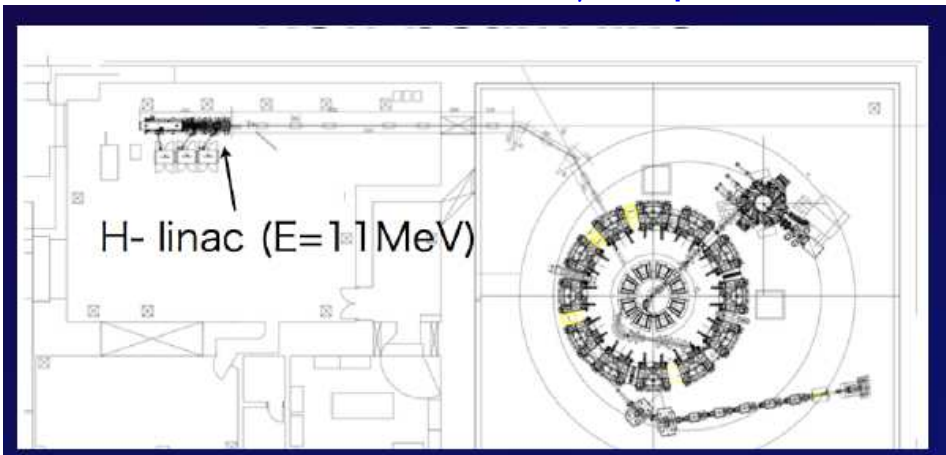


100-150 MeV proton, repetition rate 20-50 Hz

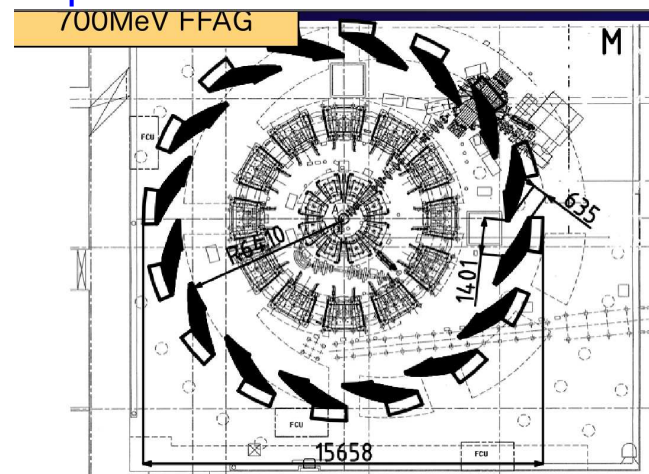


• Upgrades :

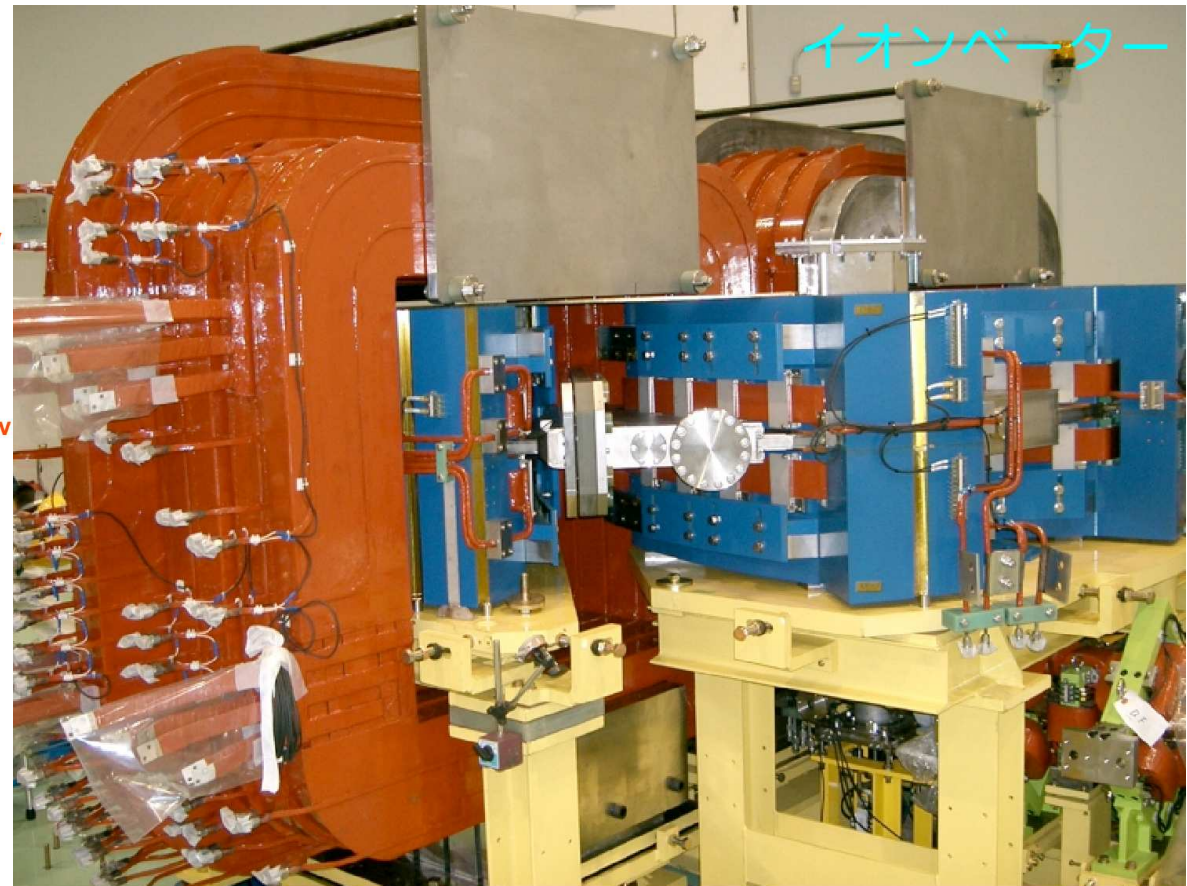
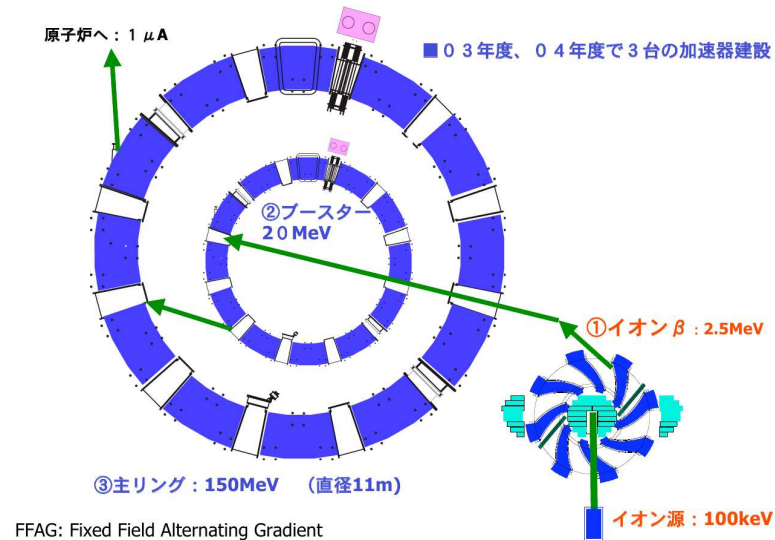
On-going : H- charge exchange injection
Towards 10s of μ Amp



Planned : neutron flux increased by a factor 30.
Options : additional 700 MeV spiral lattice FFAG,
or 400 MeV quasi-isochronous FFAG



KURRI KUCA 3-ring cascade



100keV	2.5MeV	20MeV
2.5MeV	20MeV	150MeV
Spiral Induction	Radial DFD	Radial DFD
rf	rf	
8	8	12
2.5	4.5	7.6
coil	pole	pole
5.00	2.84	2.83
0.60m	1.42m	4.54m
0.99m	1.71m	5.12m

The magnet gap is non-scaling : parallel faces. Pole face windings control the r-dependence of the vertical tune.

7 ERIT

- “Energy Recovery Internal Target”, at KURRI, Kyoto University.
- ◊ A compact proton storage ring for the production of 10 MeV BNCT neutrons
- ◊ High neutron flux is needed at patient : $\approx 2 \cdot 10^{13}$ neutrons in 30 minutes for typical tumor volume
- ◊ Today, a 5-10 MW reactor is used, there is needed for hospital environment compliant equipment : ERIT

Injector (425 MHz RFQ + IH-DTL)

H-, kinetic energy 11 MeV

Peak/average beam current 5 mA / $> 100\mu\text{A}$

Repetition rate 200 Hz, d.c. 2%



FFAG ring

FDF lattice, 8 cells

H- injection on internal Be target ($5 - 10\mu\text{m}$ thick)

proton energy 11 MeV

circulating current 70 mA

ERIT system

Beam survival 500-1000 turns

Target lifetime > 1 month

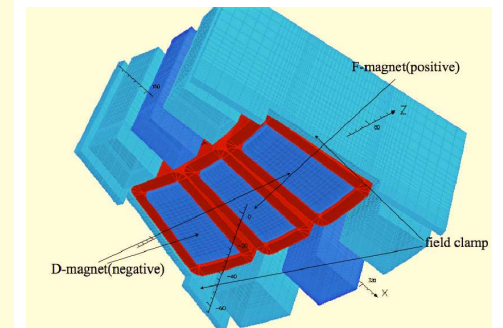
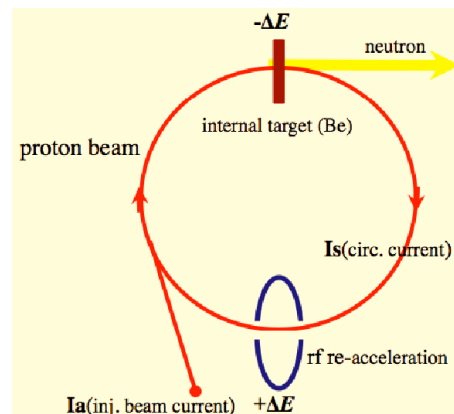
ΔE / turn 70 keV

RF cavity

Operated CW, 100 kW input power

RF voltage / frequency 250 kV / 18.1 MHz

Harmonic number 5



8 PRISM

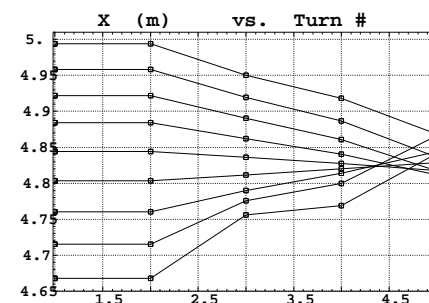
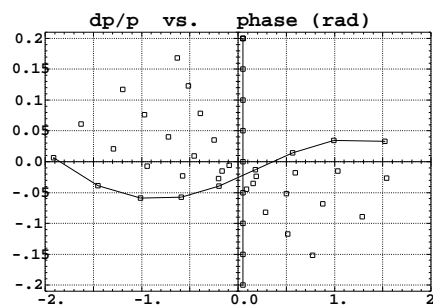
- A muon bunch phase rotator
- ◊ An R/D program started in 2003
- ◊ **FFAG used as phase rotator, for momentum compression**

$p=68\text{MeV}/c$ +/-20% down to +/-2% in 6 turns

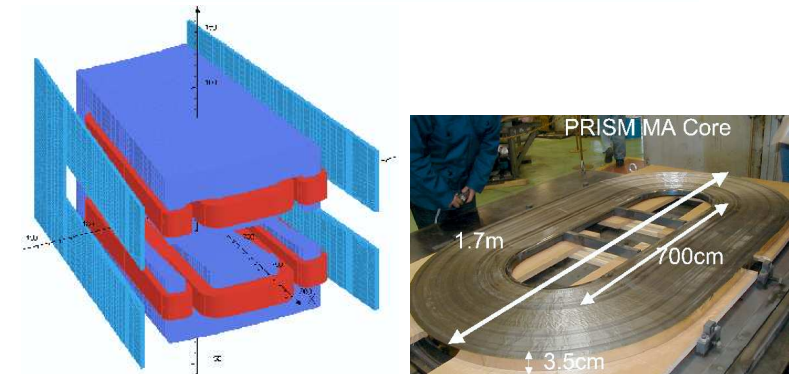
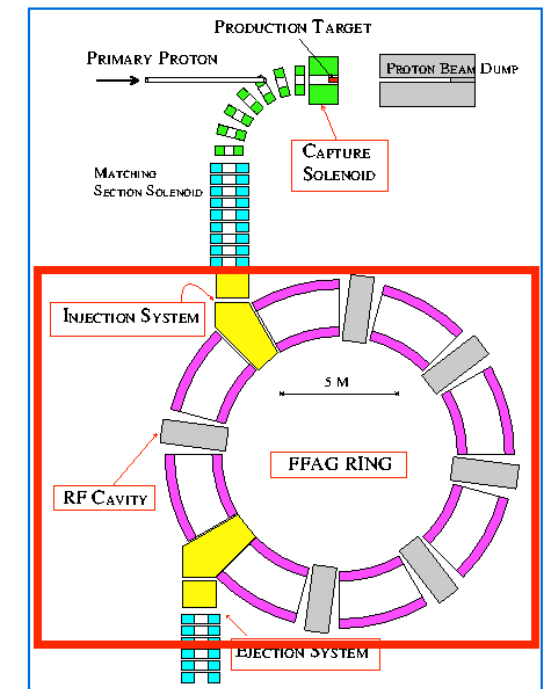
Advantage of FFAG optics : large geometrical acceptance, zero chromaticity

A difficult task : injection and extraction

- ◊ FFAG ring characteristics :
- DFD lattice 14t triplet yoke, 120 kW/triplet
- $K, B_F/B_D$ variable → quasi-decoupled ν_x, ν_z adjustments
- H / V apertures : 1 / 0.3 m
- acceptance : $4\pi \text{ cm.rad} \times 0.65\pi \text{ cm.rad}$
- RF : 5-gap cavity, 33 cm gap, 150-200 kV/m, 2MV/turn, saw-tooth waveform



- ◊ 2005: downsized to 6 cells for POP,
- central orbit radius 3 meter
- 2.1 MHz ($h=5$) RF, gap voltage 33 kV peak
- operated using 100 MeV/c alphas from an ^{241}Am source.



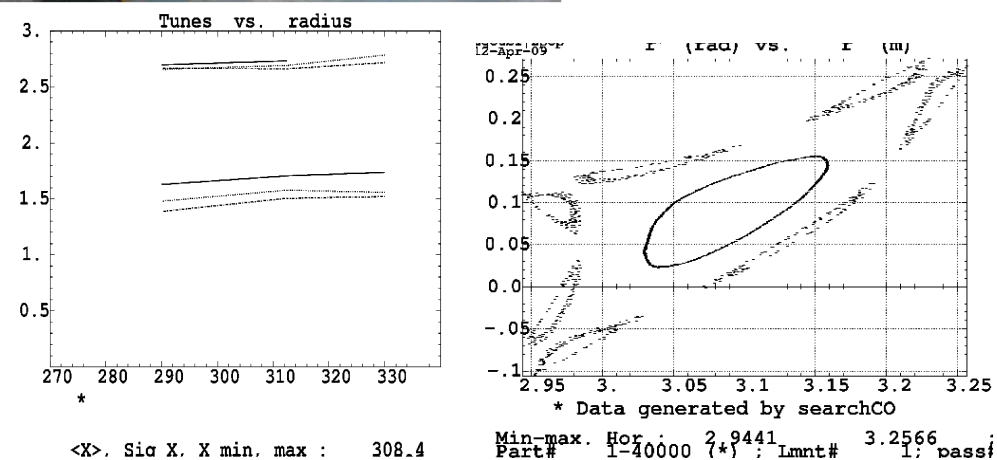
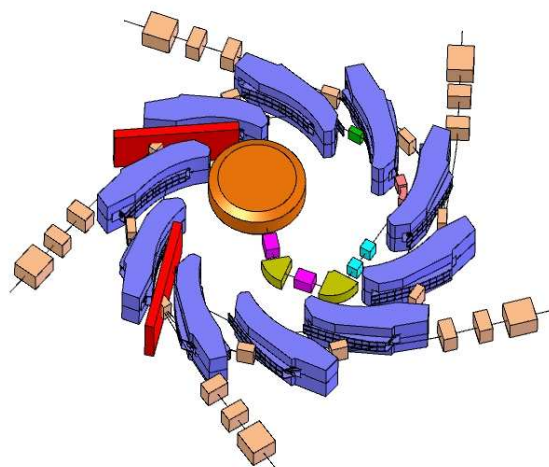
9 RACCAM

- Working frame : Neutrino factory R/D and medical applications.
French ANR funding, 2006-2008.
- A feasibility study of a rapid-cycling, variable energy, spiral lattice scaling FFAG
- Magnet prototype (built by SIGMAPHI) proved
 - gap shaping spiral sector
 - scaling FFAG field, including flutter

Tracking in measured field maps (3D Hall-probe, by SIGMAPHI) proved

- constant tunes
- large dynamical aperture

- Outcome :
 - demonstration of gap shaping scaling spiral dipole feasibility. **First of the kind.**
 - a cost-effective multiple-beam delivery hadrontherapy installation.



10 Straight S-FFAG line

- ◊ Scaling FFAG accelerators can be designed not only in a ring shape, but also with no overall bend.
- ◊ This requires a mid-plane guide field of the form

$$B_y(x, s) = B_0 e^{m(x-x_0)} F(s)$$

- ◊ Similarly to the cylindrical (r, θ) case, B_0 is some reference field value, taken at some arbitrary reference x_0 , $F(s)$ is a flutter function.

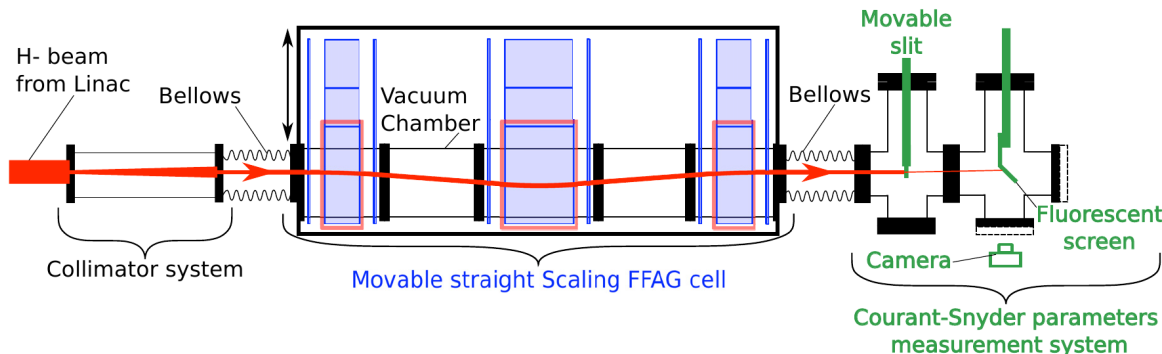
$m = \frac{\rho}{B_0} \frac{\partial B}{\partial x}$ is the normalized field gradient.

The experiment used the 11 MeV linac (injector of the 150 MeV FFAG). The FDF cell is moved horizontally (bellows) to match the incident beam momentum to the proper FFAG orbit.

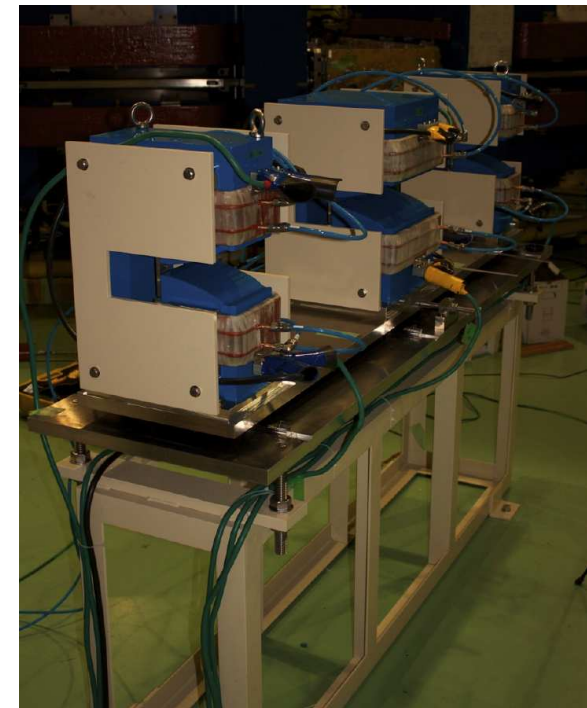
The experiment measured the orbit location, optical functions including phase advances, for various momenta, and showed good agreement with outcomes of tracking in field maps.

TUPPC022

Proceedings of IPAC2012, New Orleans, Louisiana, USA



Type	FDF
<i>m</i> -value	11 m^{-1}
Total length	4.68 m
Length of F magnet	15 cm
Length of D magnet	30 cm
Max. B Field	0.35 T
Horizontal phase advance	87.7 deg.
Vertical phase advance	106.2 deg.



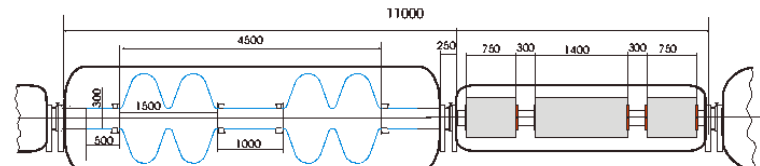
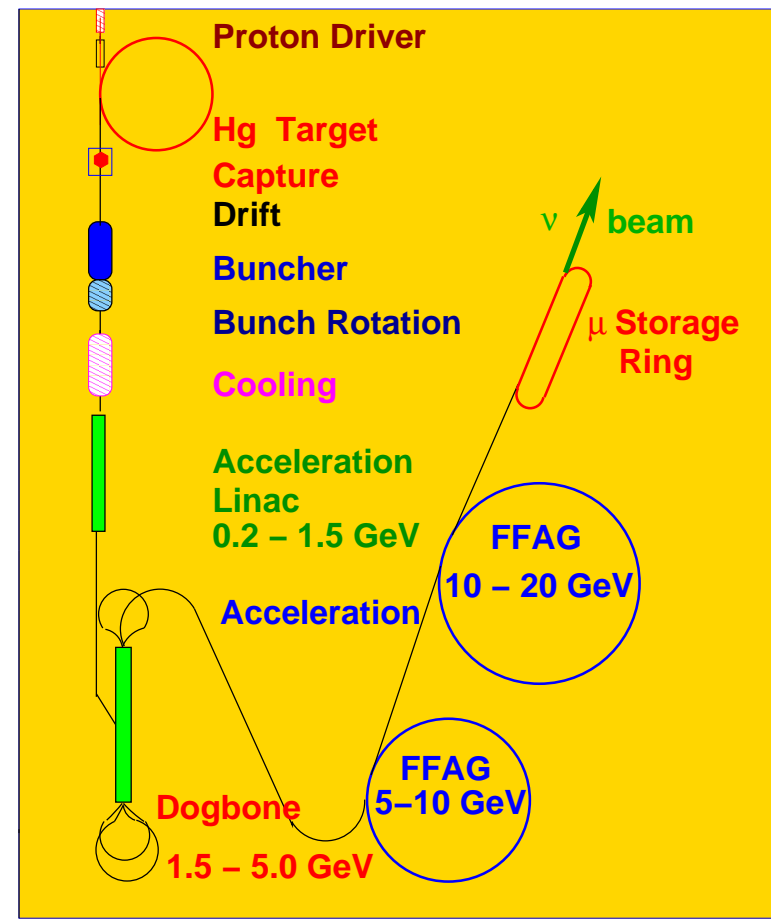
11 EMMA

Back to the neutrino factory, US-Study-2a : based on linear FFAG

- FFAG based on linear optical elements (quadrupoles)
- orbits no longer scale, tunes are allowed to vary with energy

This has a series of consequences :

- $R/\rho < 2$ - this decreases the machine size compared to classical (scaling) FFAG
- horizontal beam excursion is reasonable (small D_x)
→ magnets apertures are much smaller
- yields **large transverse acceptance** ← fields are linear ($3\pi\text{cm}$ achieved)
- small δTOF over energy span, allows **fast acceleration** high gradient RF (200 MHz type SCRF cavities)
- Above 5 GeV, non-scaling linear FFAG method yields **lower cost/GeV than RLA**.

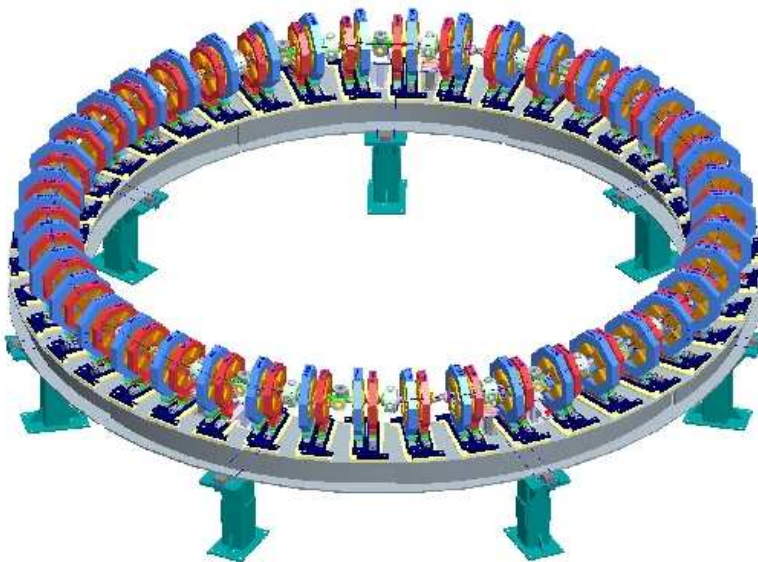


• The EMMA experiment.

◊ An experimental model to investigate the new concept of “linear FFAG” :

- linear magnets (quadrupoles) → yields huge acceptance
- fixed field → yields fast acceleration
- fast acceleration → requires a lot of RF, and fixed frequency, gutter acceleration

- Launched in the frame of Neutrino Factory R&D
 - An experimental model of muon accelerators
 - International collaboration :
- BNL, CERN, FNAL, LPSC, STFC, J.Adams Inst., Cockcroft Inst., TRIUMF**
- Recollection :
- 1999 : principle of linear FFAG optics, FNAL**
2001 : first e-model meeting, BNL
2006 : project funded by “British Accelerator Science and Radiation Oncology Consortium”, 3.5 years : 04-2007 / 09-2010, £5.6M budget
- Construction started at Daresbury, 04/2007, first beam planned summer 2009



*A model of Study IIa FFAG
10 to 20 MeV
42 cells, doublet
pole-tip fields ≈ 0.2 T
apertures $\approx \phi 40$ mm
37cm cell length
16m circumference
1.3GHz RF
1 cavity every other cell*

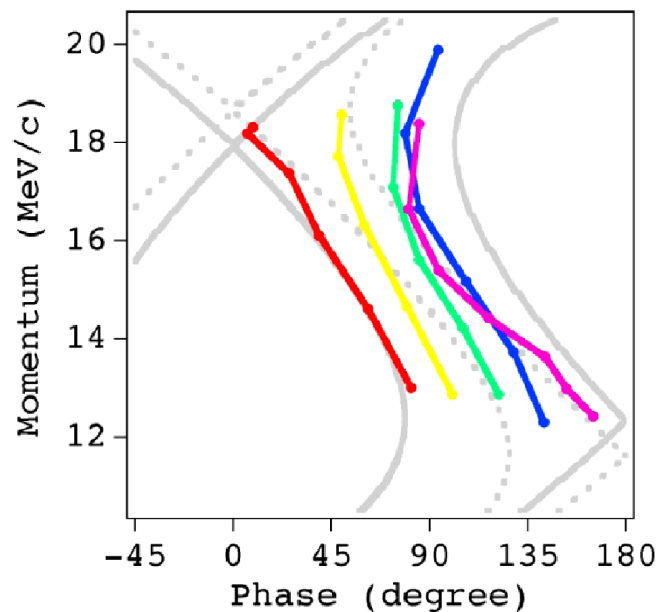


- Construction at Daresbury Lab. started in 2007
- Commissioning started in 2010
- “Serpentine” acceleration demonstrated in 2011



EMMA parameters

Energy range	<i>MeV</i>	10 - 20
number of turns		<16
circumference	<i>m</i>	16.568
Lattice		F/D doublet
No of cells		42
RF frequency	<i>GHz</i>	1.3
No of cavities		19
RF voltage	<i>kV/cav.</i>	20 - 120
RF power	<i>kW/cav.</i>	<2
Rep. rate	<i>Hz</i>	1-20

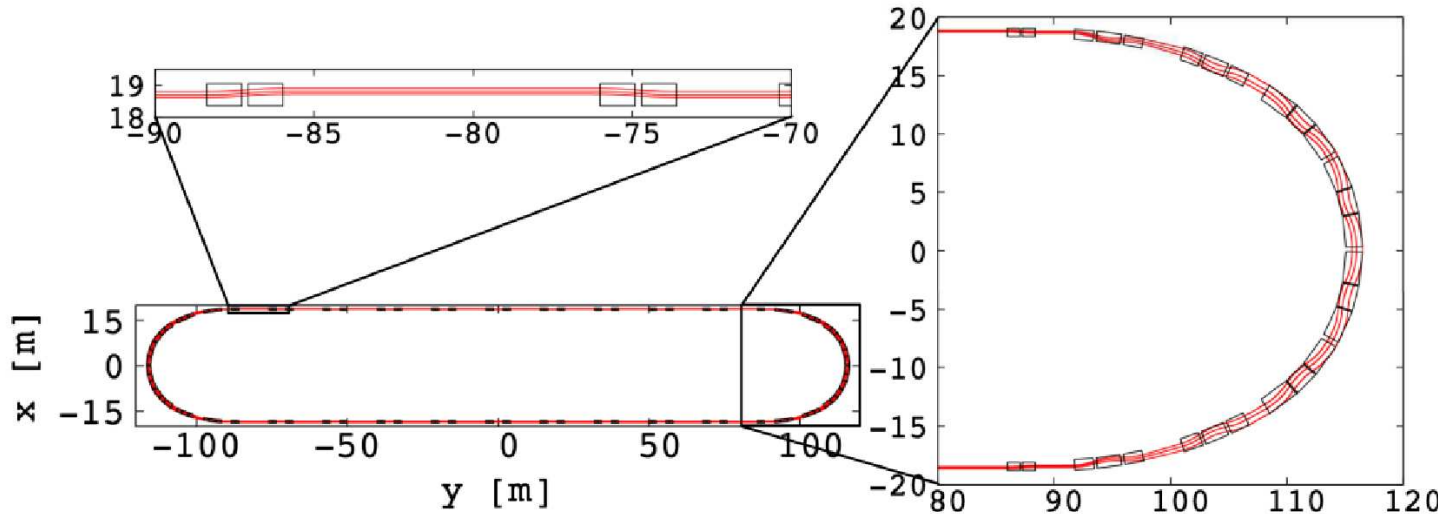


12 A bestiary of FFAG design studies

A *very limited* excerpt of what can be found in our Labs... See the bibliography for more, in particular the FFAG workshops.

- **nuSTORM FFAG decay ring, J.-B. Lagrange et al. [IPAC2016]**

- ◊ Neutrinos from STORed Muon beam (nuSTORM), the simplest implementation of a neutrino factory : pions are directly injected into a racetrack storage ring, where the circulating muon beam is captured.



- ◊ The racetrack nuSTORM FFAG lattice with zoom on the straight section (top left) and on the arc section (right).
- ◊ The muon flux is key to successful neutrino experiment, so, FFAG optics allows ring with large momentum acceptance, $\sim \pm 20\%$.
straight section to avoid activation in the arc.

- **Vertical FFAG [S. Brooks, PRST AB 16, 084001 (2013)]**

- ◊ Vertical scaling optics was devised by K. Ohkawa (once known as the “smokatron”),
- ◊ Re-investigated recently [S. Brooks, prst-ab]

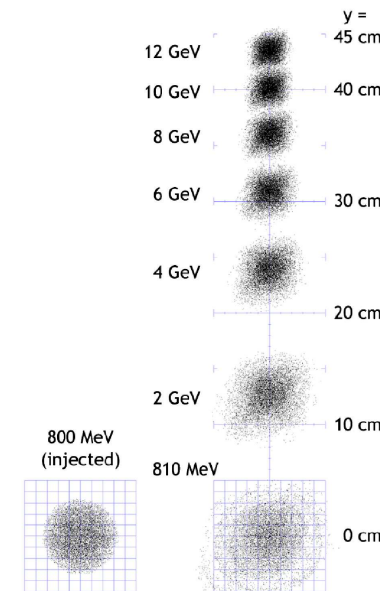
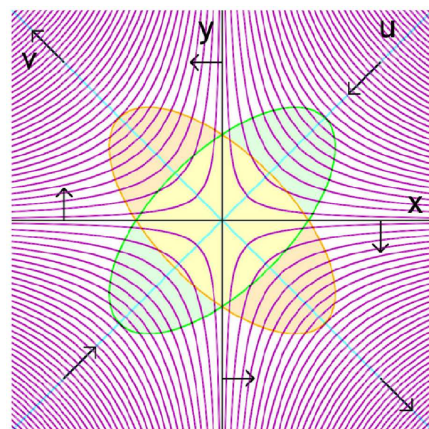
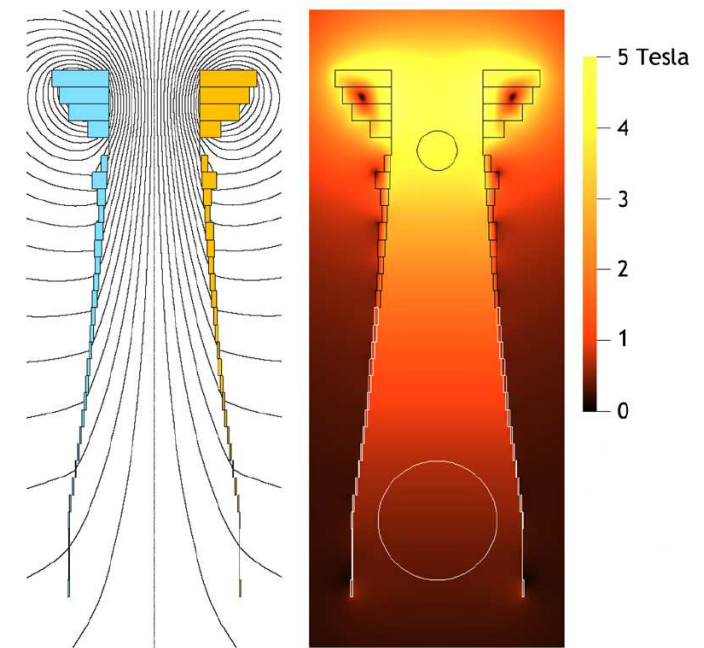
Field on closed orbit in a scaling VFFAG magnet:

$$B_0 \exp(ky)$$

Momentum dependence of vertical orbit position:

$$y = \frac{1}{k} \ln \frac{p}{p_{inj}}$$

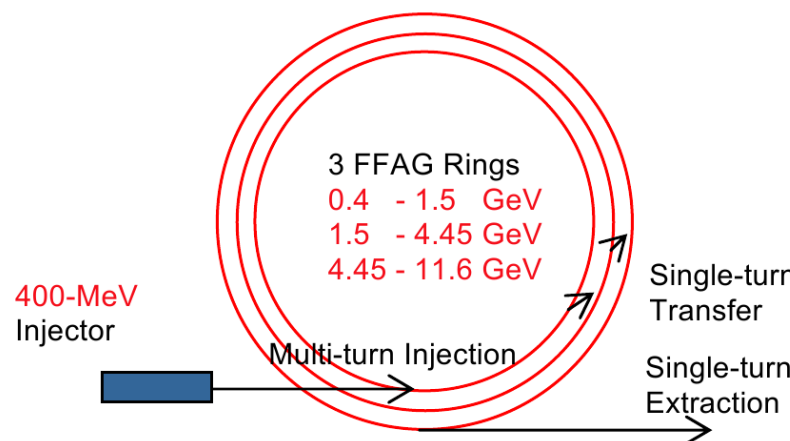
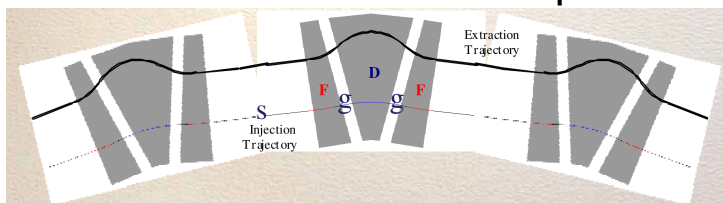
Path-length is constant. Relativistic motion is isochronous.



- A linear FFAG proton-driver design [S. Ruggiero, BNL, 2004]

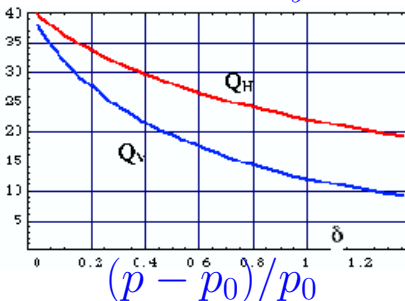
- ◊ A 3-stage linear FFAG cascade, as a NuFact p-driver

- ◊ Linear FDF FFAG triplet



- ◊ Fast resonances crossing :

$$Q_x : 40 \rightarrow 19, \quad Q_y : 38 \rightarrow 9.$$



- ◊ Neutrino factory p-driver parameters :

		Ring 1	Ring 2	Ring 3
Energy, Inj.	(GeV)	0.4	1.5	4.5
Extr.	(GeV)	1.5	4.5	12
# of turns		1800	3300	3600
cycle time	ms	6	9	10
Circumf.	m	807	819	831
# cells		136	136	136
cell length	(m)	5.9	6	6.1
h		136	138	140
RF freq.	MHz	36-46	46-49.7	49.7-50.4
E gain / turn	MeV	0.6	0.9	2

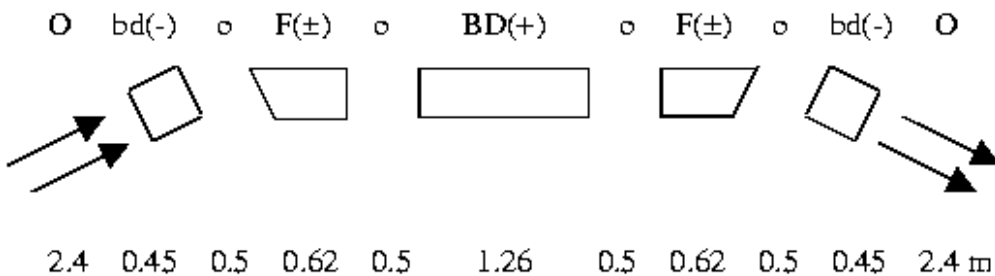
- ◊ Operation mode variant considered for ring #1, for ~MW beam power in GeV range :
 - broad-band, few MHz RF (JPARC style), cycled,
 - repetition rate > 100 Hz,
- ◊ Even higher rep. rate. (toward CW) based on
 - “harmonic number jump”,
 - using high frequency fixed-frequency RF.
 Requires cavity with transverse RF voltage profile.

• Pumplet lattice [G. Rees, RAL]

- A non-linear, non-scaling type of FFAG, isochronous
- A scheme investigated for a 20 GeV, 4 MW proton driver for the neutrino factory

◊ The many knobs (field non-linearities) allow isochronism

Lattice for 8 to 20 GeV / 16 turns / 123 cell ring :



$$B_{bd}(x) = -3.456 - 6.6892 x + 9.4032 x^2 - 7.6236 x^3 + 360.38 x^4 + 1677.79 x^5$$

$$B_{BF}(r) = -0.257 + 16.620 r + 29.739 r^2 + 158.65 r^3 + 1812.17 r^4 + 7669.53 r^5$$

$$B_{BD}(x) = 4.220 - 9.659 x - 45.472 x^2 - 322.1230 x^3 - 5364.309 x^4 - 27510.4 x^5$$

Allows insertion straights - advantages :

1. easier injection and extraction,
2. space for beam loss collimators,
3. RF gallery extending only above the insertions, not above the whole ring,
4. 4-cell cavities usable, thus reducing, by a factor of four, the total number of rf systems.

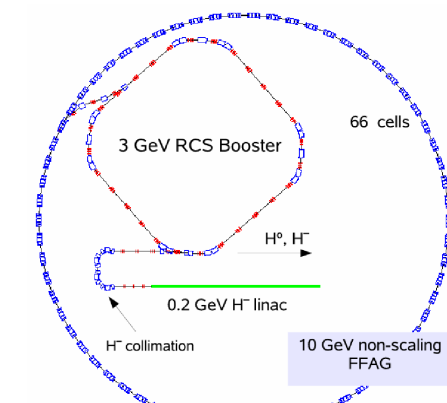
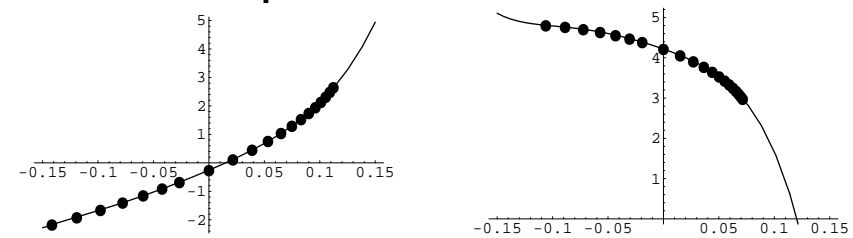
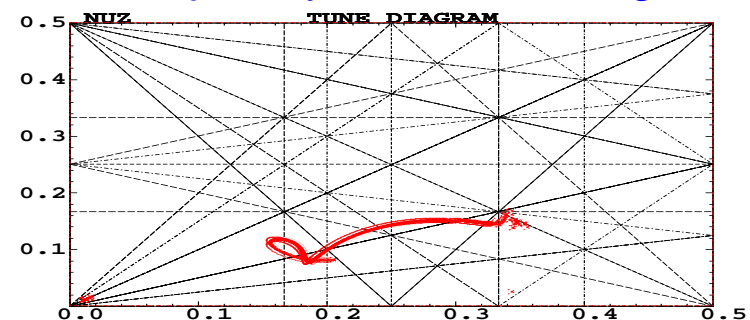


Figure 1: Layout drawing of the 4 MW, NFFAG driver.

◊ Field profile in BF and BD :



◊ Beam trajectory in the tune diagram :



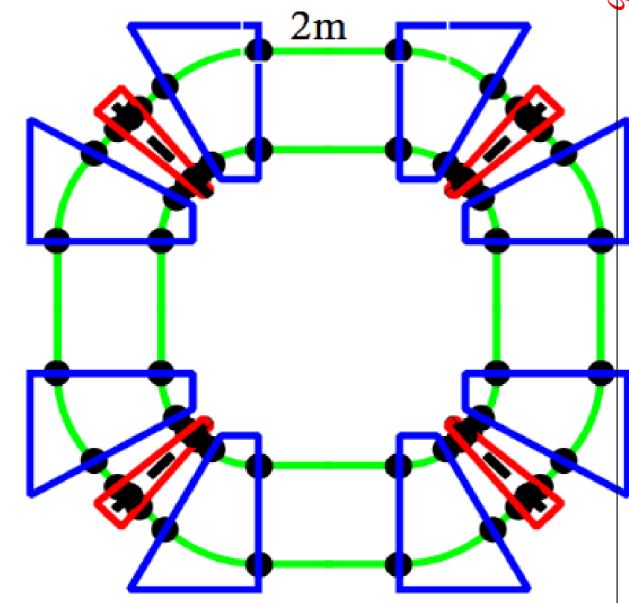
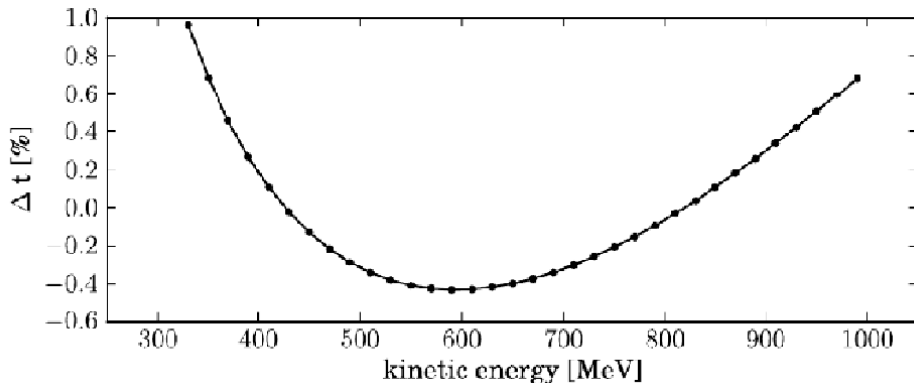
- Toward CW [C. Johnstone, FNAL]

Quasi-isochronous optics,

- ◊ based on SC dipoles and featuring
 - alternating-gradient with non-linear radial field profile
 - optimized magnet-edge contour
- ◊ Allows near-crest (serpentine) acceleration, based on SCRF

◊ Principle 6-cell lattice used for numerical beam dynamics studies :

0.33 to 1 GeV at a rate of 10~20 MV/turn



- ◊ Numerical beam dynamics studies show
 - large transverse dynamical acceptance
 - currents in 20 mA range with no transverse beam growth doable (OPAL simulations)

- Serpentine acceleration in scaling lattice, FFFFAG [E. Yamakawa et al., KURRI]

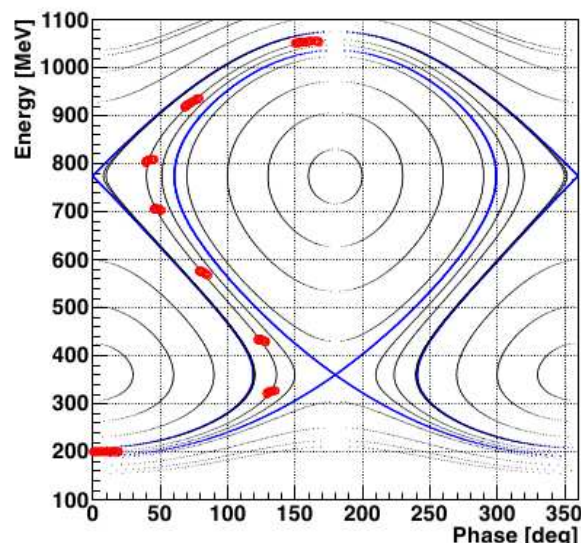
- ◊ The lattice $\gamma_{\text{tr}} = \sqrt{1 + K}$ is set to be in the acceleration range : beam γ is accelerated in transition region, time of flight is parabolic
- ◊ This allows using fixed RF-frequency acceleration in variable $\beta = v/c$ regime
- i.e., case of non-relativistic beam, suitable for proton acceleration.

- ◊ An ADS equivalent has been designed
(NIM A 716 (2013))

- ◊ Experimental demonstration performed with an electron prototype (Japan, 2012):

- small e-beam ring
- 160 keV → 8 MeV
- F-D-F scaling triplet lattice at transition gamma (764 keV)
- RF freq. 75 MHz (h=1), 750 kV/gap

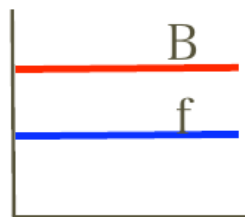
<i>k</i> -value	1.45
Equivalent mean radius at 200 MeV [m]	3
Equivalent mean radius at 1 GeV [m]	5.9
Stationary kinetic energy below transition [MeV]	360
rf voltage [MV/turn]	15 (h=1)
rf frequency [MHz]	9.6(h=1)



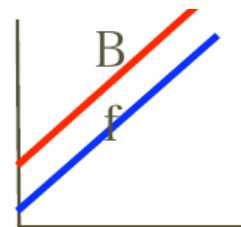
And today ...

More going on !

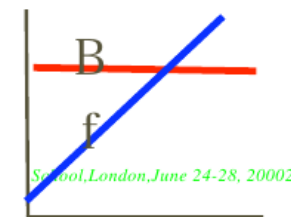
THANK YOU FOR YOUR ATTENTION



accelerating time



accelerating time



accelerating time

